

Dp-brane dynamics and thermalization in type IIB Ben Ami-Kuperstein-Sonnenschein models

Dariusz Kaviani*

School of Particles and Accelerators, Institute for Research in Fundamental Sciences (IPM), P.O. Box 19395-5531, Tehran, Iran

ABSTRACT: We study the world volume Hawking temperature of all type IIB rotating probe Dp -branes, dual to the temperature of different flavors at finite R-charge, in the Ben Ami-Kuperstein-Sonnenschein holographic models including the effects of spontaneous breakdown of the conformal and chiral flavor symmetry. The model embeds type IIB probe flavor Dp -branes into the Klebanov-Witten gravity dual of conformal gauge theory, with the embedding parameter, given by the minimal radial extension of the probes, setting the IR scale of conformal and chiral flavor symmetry breakdown. We show that when the minimal extension is positive definite and additional spin is switched on, the induced world volume metrics of only certain type IIB probe branes admit thermal horizons and Hawking temperatures despite the absence of black holes in the bulk. We find that the world volume black hole nucleation is non-trivial and depends on the world volume dimension and topology of the non-trivial internal cycle wrapped by the probe. We find, in addition, that by varying the minimal extension of the probe, large hierarchies of temperature scales get produced, with the temperature behavior varying dramatically, depending on the type of probe. We also derive the energy-stress tensor of the thermal probes and study their backreaction and energy dissipation. We show that at the IR scale the backreaction is non-negligible and find the energy can flow from the probes to the bulk, dual to the energy dissipation from the flavor sectors into the gauge theory.

KEYWORDS: D-branes, Brane Dynamics in Gauge Theories.

*Email: dariush@ipm.ir

Contents

1. Introduction	1
2. Review of the BKS models	8
2.1 The KW solution	8
2.2 U-like embedded probe D7-branes wrapping $adS_5 \times S^3 \subset adS_5 \times T^{1,1}$	10
2.3 U-like embedded probe D5-branes wrapping $adS_3 \times S^3 \subset adS_5 \times T^{1,1}$	12
2.4 U-like embedded probe D5-branes wrapping $adS_4 \times S^2 \subset adS_5 \times T^{1,1}$	13
2.5 U-like embedded probe D3-branes wrapping $adS_2 \times S^2 \subset adS_5 \times T^{1,1}$	14
3. Induced metric and temperature on U-like embedded probe D7-brane wrapping $adS_5 \times S^3 \subset adS_5 \times T^{1,1}$ and spinning about $S^2 \subset T^{1,1}$ with world volume electric field turned on	15
4. Induced metric and temperature on U-like embedded probe D5-brane wrapping $adS_3 \times S^3 \subset adS_5 \times T^{1,1}$ and spinning about $S^2 \subset T^{1,1}$ with world volume electric field turned on	23
5. Induced metric and temperature on U-like embedded probe D5-brane wrapping $adS_4 \times S^2 \subset adS_5 \times T^{1,1}$ and spinning about $S^3 \subset T^{1,1}$	32
6. Induced metric and temperature on U-like embedded probe D3-brane wrapping $adS_2 \times S^2 \subset adS_5 \times T^{1,1}$ and spinning about $S^3 \subset T^{1,1}$	35
7. Discussion	37

1. Introduction

Non-equilibrium steady states are of great interest in many branches of physics, such as heavy ion physics (thermalization of the quark-gluon plasma), condensed matter physics (quenches of cold atom systems), cosmology (non-equilibrium phase transitions and the Kibble-Zurek mechanism) and more. Studying such states by standard field theory techniques is prohibitively difficult (except for special cases involving conformal symmetry or integrability), however, they can be easily constructed by using probe D-brane dynamics in gauge/gravity duality.

In gauge/gravity duality, [1] (see also [2]), the pure gravity dual solution of conformal gauge theory is produced by taking the near horizon limit of N backreacting

D3-branes at a smooth point of the transverse space described by the $adS_5 \times S^5$ background metric. The extension of such holographic solution includes the addition of flavored quarks to the pure gauge theory, by embedding additional N_f flavor branes into the pure gravity dual, taking the probe limit, $N_f \ll N$, [3] (see also [2])¹. In order to construct non-equilibrium systems in such flavored holographic models, one then notes that when the flavored quark sector (dual to the probe flavor branes) attain finite temperature while the pure gauge theory itself (dual to the pure gravity solution) is at zero temperature, the system describes non-equilibrium steady states. The prime examples of such non-equilibrium steady states have been constructed in ref. [11] (see also [12, 13]), by embedding type IIB probe flavor Dp -branes ($p = 1, 3, 5, 7$) into the $adS_5 \times S^5$ gravity dual of conformal gauge theory ($\mathcal{N} = 4$ SYM). (For $p = 7$, the probe fills all the spacetime directions of the gravity dual and the corresponding gauge theory is given by conformal field theory (CFT). For $p < 7$, the probes are localized in some spacetime directions of the gravity dual and the corresponding gauge theory is given by *defect* conformal field theory (dCFT)). In ref. [11] (see also [12, 13]) rotating probe Dp -brane solutions have been constructed and shown that when spin is turned on, the induced world volume metric on *all* type IIB rotating probe Dp -branes in $adS_5 \times S^5$ admit thermal horizons and Hawking temperatures despite the absence of black holes in the bulk. By gauge/gravity duality, this means that when the flavor sector of the gauge theory gets R-charged, it becomes thermal. Since the gauge theory itself is at zero temperature, while its flavor sector, given, for instance, by a magnetic monopole ($p = 1$) or a quark ($p = 7$), is at finite temperature, it was concluded in ref. [11] such systems describe non-equilibrium steady states. However, by computing the energy-stress tensor, it has been shown in ref. [11], that the energy of the probe (defect) flavor brane will eventually dissipate into the bulk and form, with the large backreaction in the IR, a (localised) black hole in the bulk. By gauge/gravity duality, this means that the energy from the (defect) flavor sector will eventually dissipate into the gauge theory ($\mathcal{N} = 4$ SYM).

This analysis has been extended in ref. [14], by studying the induced world volume metrics on rotating probe Dp -branes ($p = 1$ – dual to magnetic monopoles), embedded in more general gauge/gravity dualities, including warped Calabi-Yau throats, refs. [15–17] (see also refs. [18] – extending these gravity duals to finite temperature systems). The gravity dual solution, given by the throat background, is produced by placing N regular D3-branes and M D5-branes (fractional D3-branes)

¹In gauge/gravity dual thermodynamics, [1] (see also [2]) the gravity dual solution of conformal gauge theory at finite temperature is produced by taking the near horizon limit of N black D3-branes described by known black hole background metric. In order to add flavored quarks to the gauge theory and study their thermal equilibrium properties, one embeds additional N_f flavor branes into the finite temperature gravity dual, taking the probe limit, $N_f \ll N$ [3] (see also [2]). Such holographic setup including probes, [4, 5], has been used to model flavor physics [3, 6], and quantum critical phenomena, [7], complementary to other works on charged adS black holes, [8]. Such phenomena have also been studied at zero temperature in refs. [9, 10].

at the generic Calabi-Yau singularity – the conifold tip point [19]. The solution then breaks some supersymmetry and conformal invariance and is QCD-like – admitting confinement and chiral symmetry breakdown in the regular IR, with the gravity dual given by the Klebanov-Strassler (KS) solution, [15], and RG cascade in the singular UV, with the gravity dual given by the Klebanov-Tseytlin (KT) solution, [16]. In the limit where the fractional D3-branes are removed, the theory is conformal, with the gravity dual given by the Klebanov-Witten (KW) solution, [17]. In ref. [14] it has been shown that in such gravity duals of QCD-like, $\mathcal{N} = 1$ gauge theories the induced world volume black hole on rotating probe D1-branes (dual to magnetic monopoles) forms not in the regular IR of the KS solution, where the theory is confining and admits conformal and chiral symmetry breakdown, but in the singular UV including KT solution, where the theory is non-confining and admits RG cascade and conformal symmetry breakdown. It has been shown in ref. [14] that the world volume black hole on rotating probe D1-branes forms about the KT conifold singularity with the world volume horizon and temperature changing dramatically with the scale of chiral symmetry breakdown. In the conformal limit of the UV including the KW solution, it has been shown in ref. [14] that the induced world volume metric on rotating probe D1-branes coincides with the BTZ black hole metric modulo the angular coordinate. It has been shown there that, in this case, the world volume horizon and temperature increase linearly and much faster with the angular velocity (dual to R-charge), compared with the world volume horizon and temperature in the non-conformal KT solution. However, it has been found there that the functional form and behavior of the world volume horizon and temperature get dramatically modified once a background gauge field from the $U(1)$ R-symmetry of the KW solution is activated. It has been shown there that, in this case, the world volume horizon equation describes that of the *adS*-Reissner-Nordström black hole modulo the angular coordinate, and that the world volume Hawking temperature admits two distinct branches: one where it decreases and another where it increases with growing horizon size, describing ‘small’ and ‘large’ black holes, respectively. However, by computing the energy-stress tensor, it has been shown in ref. [14], that the energy of the probe D1-brane will eventually dissipate into the bulk and form, with the large backreaction in the IR, a localised black hole in the bulk. By gauge/gravity duality, this means that the energy from the defect flavor sector will eventually dissipate into the gauge theory ($\mathcal{N} = 1$ SYM).

These analyses have been further extended in ref. [20], by studying thermalization of higher dimensional probe Dp -branes ($p = 7$ – dual to flavored quarks) in Kuperstein-Sonnenschein model, ref. [21] (see also refs. [22] – extending the model to finite temperature and density, and refs. [23, 24] – extending the model in the KS solution). Motivated by the Sakai-Sugimoto model, ref. [25], the model embeds the probe D7-brane(s) into the KW gravity dual, ref. [17], $adS_5 \times T^{1,1}$ with $T^{1,1} \simeq S^2 \times S^3$, of $\mathcal{N} = 1$ conformal gauge theory². The probe wraps $adS_5 \times S^3$ in $adS_5 \times T^{1,1}$ and the

²See also refs. [26] – considering holomorphic embeddings of D7-branes into the KS solution dual

transverse space is the two-sphere $S^2 \subset T^{1,1}$. The probe D7-brane then starts from the UV boundary at infinity, bends at the minimum extension in the IR, and ends up back the boundary. The probe D7-brane therefore produces a U-shape. Since the $D7$ -brane and anti $D7$ -brane differ only by orientation, the probe describes a supersymmetry (SUSY) breaking $D7$ -brane/anti $D7$ -brane pair, merged in the bulk at minimal extension. The SUSY breaking pair also guarantees tadpole cancellation on the transverse space by the annihilation of total $D7$ charge. When the minimal extension shrinks to zero at the conifold point, the embedding appears as a disconnected $D7$ -brane/anti $D7$ -brane pair. The $D7$ -brane then produces a V-shape. In the V-shape configuration, the induced world volume metric on the $D7$ -brane is that of $adS_5 \times S^3$ and the dual gauge theory describes the conformal and chiral symmetric phase. On contrary, in the U-shape configuration, the induced metric on the $D7$ -brane has no adS factor by the embedding parameter, i.e., by non-zero minimal extension,—which sets the IR scale conformal and chiral flavor symmetry breakdown—, giving the VEV deformations in the dual gauge theory³. In the setup of ref. [20], the probe has also been allowed, in addition, to rotate about the transverse $S^2 \subset T^{1,1}$ (dual to finite R-charge chemical potential). It has been shown in ref. [20] that when the embedding parameter,—the minimal radial extension of the probe—, which sets the IR scale of conformal and chiral flavor symmetry breakdown in the dual gauge theory, is positive definite and additional spin (dual to finite R-charge chemical potential) is turned on, the induced world volume metrics on rotating probe D7-branes admit thermal horizons and Hawking temperatures despite the absence of black holes in the bulk KW. It has been shown there that the world volume horizon grows from the minimal extension with the world volume temperature scale changing dramatically with the minimal extension which sets the IR scale of conformal and chiral flavor symmetry breakdown. It has also been shown there that when, in addition, the world volume gauge electric field (dual to finite baryon chemical potential) is turned on, the behavior of the world volume temperature changes dramatically with growing horizon size, describing ‘small’ and ‘large’ black holes. However, it has been shown in ref. [20] that this behavior in the world volume Hawking temperature depends, in turn, on the size of the minimal extension. It has been shown there that when the size of the minimal extension gets increased, the behavior of the temperature changes again dramatically,—describing only ‘large’ black holes. It has then been concluded in ref. [20] that since the bulk gravity dual of the $\mathcal{N} = 1$ gauge theory is at zero temperature, while the (rotating) probe brane dual to the flavor sector of the gauge theory is at finite temperature, such systems provide novel examples of non-equilibrium steady states in the gauge theory conformal and chiral flavor symmetry breakdown. However, by computing the energy–stress tensor, it has been shown in ref. [20] that the

to supersymmetric gauge theory without flavor chiral symmetry breaking, and refs. [27] – studying the backreaction of D7-branes in the KS & KW solutions.

³As discussed in §2, this setup cannot be realized in the well-used $adS_5 \times S^5$ background.

energy of the probe flavor brane will eventually dissipate into the bulk, forming, with the large backreaction in the IR, a black hole in the bulk. By gauge/gravity duality, it was thus found that the energy of the flavor sector will finally dissipate into the gauge theory conformal and chiral flavor symmetry breakdown ($\mathcal{N} = 1$ SYM).

The aim of this work is to extend and generalize such previous analysis and study different non-equilibrium systems and their energy flow in holographic models dual to *dCFTs* with spontaneous breakdown of the conformal and chiral flavor symmetry.

The model we consider consists of the Ben Ami–Kuperstein–Sonnenschein (BKS) holographic model, [28] (see also ref. [29] – extending the model to finite temperature and density). Motivated by the Kuperstein–Sonnenschein model, ref. [21], the model embeds type IIB probe (defect) flavor Dp -branes ($p = 3, 5$) into the KW gravity dual, ref. [17], $adS_5 \times T^{1,1}$ with $T^{1,1} \simeq S^2 \times S^3$, of $\mathcal{N} = 1$ conformal gauge theory. (The model also embeds type IIA (defect) probe flavor Dp -branes (i.e. $p = 4$) into the ABJM gravity dual, [30])⁴. In the example of probe D3-brane, the probe wraps $adS_2 \times S^2$ in $adS_5 \times T^{1,1}$ and the transverse space is the three-sphere $S^3 \subset T^{1,1}$. In the example of the probe D5-brane, there are two cases: The probe either wraps $adS_3 \times S^3$ in $adS_5 \times T^{1,1}$ and the transverse space is the two-sphere $S^2 \subset T^{1,1}$, or it wraps $adS_4 \times S^2$ in $adS_5 \times T^{1,1}$ and the transverse space is the three-sphere $S^3 \subset T^{1,1}$. In all examples, the probe Dp -brane starts from the UV boundary at infinity, bends at minimal extension in the IR, and ends up at the boundary. The probe Dp -brane thus produces a U-shape. Since the Dp -brane and anti Dp -brane differ only by orientation, the probe describes a supersymmetry (SUSY) breaking Dp -brane/anti Dp -brane pair, merged in the bulk at minimal extension. The SUSY breaking pair also guarantees tadpole cancellation on the transverse space by the annihilation of total Dp charge. When the minimal extension shrinks to zero at the conifold point, the embedding appears as a disconnected Dp -brane/anti Dp -brane pair. The Dp -brane then produces a V-shape. In the V-shape configuration, the induced world volume metric on the Dp -brane is that of $adS_m \times S^n$ and the dual gauge theory describes the conformal and chiral symmetric phase. On contrary, in the U-shape configuration, the induced metric on the Dp -brane has no adS factor by the embedding parameter, i.e., by non-zero minimal extension, –which sets the IR scale conformal and chiral flavor symmetry breakdown–, giving the VEV deformations in the dual gauge theory⁵. Here, in our setup, we let, in addition, the probe(s) rotate about the transverse S^2 or $S^3 \subset T^{1,1}$ and turn on, in addition, the world volume gauge electric field (dual to finite R-charge and density chemical potential).

The motivation is the fact that in such model the induced world volume metrics on the rotating probe branes, *if* given by black hole geometries, are then expected to give the Hawking temperatures of the probes dual to the temperatures of *defect* flavors in the dCFT with spontaneous breakdown of the conformal and chiral flavor

⁴In this paper, we will not consider such type IIA probe brane configurations.

⁵As discussed in §2, this setup cannot be realized in the well-used $adS_5 \times S^5$ background.

symmetry. Since the gauge field theory itself is at zero temperature while its flavor sector is at finite temperature, such systems exemplify novel non-equilibrium steady states in the dCFT with conformal and chiral flavor symmetry breakdown. However, interactions between different sectors are expected. The energy-stress tensor of the thermal probes is then expected to yield the energy dissipation from the probes into the system, dual to the energy dissipation from the flavor sectors into the gauge theory. We are also interested in modifying our analysis by turning on world volume gauge fields on the probe branes, – including finite baryon density chemical potential –, corresponding to turning on external fields in the dual gauge theory. The motivation is the fact that in the presence of such fields the R-symmetry of the gauge theory gets broken⁶ and the corresponding modifications in the induced metrics and energy-stress tensors of the probes are expected to reveal new features of thermalization.

The main results we find are as follows. We find that when the probe embedding is U-like, the induced world volume metrics of *only certain* type IIB rotating probe flavor Dp -branes embedded in the KW gravity dual of CFT ($\mathcal{N} = 1$ SYM) with spontaneous breakdown of the conformal and chiral flavor symmetry admit thermal horizons and Hawking temperatures of expected features despite the absence of black holes in the bulk KW⁷. We find that when the embedding is U-like, world volume black hole formation on type IIB rotating probe flavor Dp -branes embedded in the KW gravity dual of CFT, with spontaneous breakdown of the conformal and chiral flavor symmetry, depends on the world volume dimension and topology of the non-trivial internal cycle wrapped by the probe. We find that when the embedding parameter, the minimal extension of the probe, changes, the world volume black hole temperature of both spacetime filling ($p = 7$) and defect flavor branes ($p = 5$) changes dramatically, setting large hierarchies of temperature scales, while leaving the temperature behaviors unchanged. We find, however, that when the world volume electric field is turned on, the behavior of the world volume temperature of both probe flavor branes ($p = 5, 7$) changes dramatically, while the temperature scales set moderate hierarchies. We find that in the presence of the electric field the world volume temperatures of the U-like embedded probe flavor branes admit two distinct branches: there is one branch where the temperatures increase and another where they decrease with growing horizon size, corresponding to ‘large’ and ‘small’ black holes, respectively. However, by examining the parameter dependence of the black hole solutions, we find, in the case of spacetime filling flavor brane, this temperature

⁶We note that earlier studies in gauge/gravity, [31], have shown this result.

⁷This is in contrast with the main result of ref. [11] where it has been shown that in the $adS_5 \times S^5$ gravity dual of CFT ($\mathcal{N} = 4$ SYM) the induced world volume metrics of *all* type IIB rotating probe flavor Dp -branes admit thermal horizons and Hawking temperatures of expected features despite the absence of black holes in the bulk. At this point, we note again that $adS_5 \times S^5$ contains no non-trivial cycle and admits no U-like embeddings – admitting spontaneous breakdown of the conformal and chiral flavor symmetry.

behavior parameter dependent, unlike in the case of defect flavor branes where we find the temperature behavior parameter independent. We find that when the minimal extension gets increased, the world volume temperature of the spacetime filling flavor brane ($p = 7$) changes its behavior again dramatically, admitting only one class of black hole solution, including ‘large’ black holes, whereas that of the defect flavor brane ($p = 5$) remains unchanged. By gauge/gravity duality, we thus find that when the IR scale of symmetry breakdown is positive definite and the flavor sector gets R-charged, flavor thermalization and non-equilibrium steady state formation in the KW (d)CFT with spontaneous conformal and chiral symmetry breakdown is non-trivial and depends on the type of flavors inserted into the gauge theory. By gauge/gravity duality, we also find that the temperature of both spacetime filling and defect flavored quarks varies dramatically with the IR scale of conformal and chiral flavor symmetry breakdown, which sets large hierarchies of temperature scales, while leaves the temperature behaviors unchanged. By gauge/gravity duality, we find, however, that when the external electric field is turned on, the temperature behavior of both spacetime filling and defect flavored quarks changes dramatically. In this case, we find, however, that when, in addition, the IR scale increases, the temperature behavior of spacetime filling flavored quarks changes again dramatically, but that of defect flavors remains unchanged. However, by computing the energy–stress tensor of the U-like embedded rotating probe flavor Dp -branes, we find that, in any case, the energy of both spacetime filling and defect probe flavor branes will eventually dissipate into the bulk and form, with the large backreaction in the IR, a black hole in the bulk. By gauge/gravity duality, we thus find that the energy from both spacetime filling and defect flavor sectors will eventually dissipate into the $\mathcal{N} = 1$ gauge theory conformal and chiral flavor symmetry breakdown.

The paper is organized as follows. In Sec. 2, we review the basics of the type IIB BKS holographic models. We first review very briefly the basics of the KW solution and write down the specific form of the background metrics and probe Dp -brane action used in the BKS models. We then review the BKS models constructing U-like embedded probe Dp -brane ($p = 3, 5, 7$) solutions in KW. In Secs. 3 – 6, we modify the BKS models by turning on spin and world volume electric field on the probe Dp -branes. In Sec. 3, we first derive the induced world volume metric and Hawking temperature on the probe $D7$ -brane wrapping $adS_5 \times S^3 \subset adS_5 \times T^{1,1}$ and rotating about $S^2 \subset T^{1,1}$. We then derive the energy–stress tensors of the rotating $D7$ -branes and compute their backreaction and energy dissipation. In Sec. 4, we do the same computations for the probe $D5$ -branes wrapping $adS_3 \times S^3 \subset adS_5 \times T^{1,1}$ and rotating about $S^2 \subset T^{1,1}$. In Sec. 5, we do the same computations for the probe $D5$ -branes wrapping wrapping $adS_4 \times S^2 \subset adS_5 \times T^{1,1}$ and rotating about $S^3 \subset T^{1,1}$. In Sec. 6, we do the same calculations for the probe $D3$ -brane wrapping $adS_2 \times S^2 \subset adS_5 \times T^{1,1}$ and rotating about $S^3 \subset T^{1,1}$. In Sec. 7, we summarize and discuss our results with future outlook.

2. Review of the BKS models

2.1 The KW solution

The particular ten-dimensional holographic string solution we are interested in is the KW solution, [17], resulting from taking the near horizon limit of a stack of N background D3-branes on the conifold point. The conifold is a singular and non-compact Calabi-Yau three-fold described, in terms of complex coordinates $z_n \in \mathbb{C}^4$, by the constraint and three-form as:

$$\sum_{n=1}^4 z_n^2 = 0, \quad \Omega = \frac{dz_2 \wedge dz_3 \wedge dz_4}{z_1}. \quad (2.1)$$

The constraint equation in (2.1) describes a singular non-compact cone with symmetry $SO(4) \times U(1) \simeq SU(2) \times SU(2) \times U(1)$, and the three-form in (2.1) is charged under the $U(1)$ R-symmetry. The base of the cone is a five-dimensional Einstein manifold, $X_5 = T^{1,1}$, of topology $SO(4)/U(1) \simeq SU(2) \times SU(2)/U(1)$, which can be identified by intersecting the constraint in (2.1) with the unit three-sphere $\sum_{n=1}^4 |z_n|^2 = 1$.

The constraint equation in (2.1) can recast its form as:

$$\det_{i,j} z_{ij} = 0, \quad \text{with} \quad z_{ij} = \sum_n \sigma_{ij}^n z_n. \quad (2.2)$$

Here σ^n denote the Pauli matrices with $n = 1, 2, 3$ and $\sigma^4 = i\mathbf{I}$. To solve Eq. (2.2), one may use unconstrained variables $z_{ij} = a_i b_j$, where a_i, b_j denote complex scalars with $i, j = 1, 2$. These scalars poses an additional $SU(2) \times SU(2)$ global symmetry, which is quotiented by the $U(1)$ symmetry via $a_i \rightarrow \exp(i\alpha) a_i$ and $b_j \rightarrow \exp(-i\alpha) b_j$, so that the global symmetry is $SU(2) \times SU(2)/U(1)$.

To construct the gauge field theory of the solution, one may use a_i, b_j and notes the following points. First, since the conifold is a Calabi-Yau manifold, it preserves by the virtue of Killing spinor equations, one quarter of the original supersymmetry. Thus the solution has $\mathcal{N} = 1$ supersymmetry and one may associate chiral $\mathcal{N} = 1$ superfields A_i, B_j with $i, j = 1, 2$ to the complex scalars a_i, b_j . Second, further to the $SU(2) \times SU(2)/U(1)$ global symmetry discussed above, the solution has a $U(1)_R$ symmetry. Third, the field theory exemplifies a quiver gauge theory. Namely, the field theory of N D3-branes placed on the conifold tip point has a $SU(N) \times SU(N)$ gauge symmetry where A_i and B_j transform in the $(\mathbf{N}, \overline{\mathbf{N}})$ and $(\overline{\mathbf{N}}, \mathbf{N})$ representation, respectively. Fourth, anomaly cancellation in $U(1)_R$ requires A_i and B_j have R-charge $1/2$, respectively. Thus the gauge theory also includes a marginal superpotential $W = \epsilon^{ij} \epsilon^{kl} \text{Tr} A_i B_k A_j B_l$ which is uniquely fixed by the symmetries modulo an overall factor.

To construct the gravity dual of this gauge theory, one notes that Eq. (2.2) describes a cone over the base of coset space $T^{1,1} = SU(2) \times SU(2)/U(1)$. One also

notes that the z_{ij} can be explicitly parameterized by five Euler angles (ψ, ϕ_i, θ_i) with $i = 1, 2$ (not written out here) whereby the metric on the conifold then takes the form [19]:

$$ds_{T^{1,1}}^2 = \frac{1}{9} \left(d\psi + \sum_{i=1}^2 \cos \theta_i d\phi_i \right)^2 + \frac{1}{6} \sum_{i=1}^2 (d\theta_i^2 + \sin^2 \theta_i d\phi_i^2). \quad (2.3)$$

Here $0 \leq \psi \leq 4\pi$, $0 \leq \phi_i \leq 2\pi$ and $0 \leq \theta_i \leq \pi$. It is clear from (2.3) that the $T^{1,1}$ base is a S^1 bundle over $S^2 \times S^2$. It is also clear from (2.3) that the $T^{1,1}$ base has the topology $S^2 \times S^3$ where the three-cycle S^3 can be parameterized by $\theta_1 = \phi_1 = 0$ and the two-cycle S^2 by $\psi = 0$, $\theta_1 = \theta_2$, $\phi_1 = -\phi_2$, with both S^2 and S^3 shrinking to zero size at the tip of the cone.

The alternative way of writing the metric on the conifold is [32]:

$$ds_{T^{1,1}}^2 = \frac{r^2}{3} \left[\frac{1}{4} (\Omega_1^2 + \Omega_2^2) + \frac{1}{3} \Omega_3^2 + \left(d\theta - \frac{1}{2} \Omega_2 \right)^2 + \left(\sin \theta d\phi - \frac{1}{2} \Omega_1 \right)^2 \right]. \quad (2.4)$$

Here r is the radial coordinate of the conifold (2.1), θ and ϕ parameterize the S^2 , and Ω_i are one-forms parameterizing the S^3 . The Ω_i s can be represented by Maurer-Cartan one-forms w_i via two $SO(3)$ matrices (not written out here) parameterized by θ and ϕ , respectively, which show that the S^3 is fibered trivially over the S^2 .

Taking the near-horizon limit of N D3-branes at the tip of the cone over $T^{1,1}$, gives the gravity dual, $adS_5 \times T^{1,1}$, of the $\mathcal{N} = 1$ superconformal gauge field theory described by the superfields A_i, B_i and the superpotential W , as above. The full ten-dimensional warped background metric takes the form [17]:

$$ds_{10}^2 = \frac{r^2}{L^2} dx_n dx^n + \frac{L^2}{r^2} (dr^2 + r^2 ds_{T^{1,1}}^2). \quad (2.5)$$

Here the first term in (2.5) is the usual four-dimensional Minkowski spacetime metric, the second term is the metric on the conifold, given either by (2.3) or by (2.4), and $L^4 \equiv (27\pi/4)g_s N(\alpha')^2$. In order to have a valid supergravity solution, (2.5), the number of D3-branes, N , has to large and the string coupling, g_s , has to be small, so that $g_s N \gg 1$; $\alpha' = l_s^2$ denotes the string scale. Here the dilaton is constant, and the other non-trivial background field is a self-dual R-R five-form flux (not written out here).

To add flavored quarks to the pure conformal gauge field theory, one embeds probe flavor Dp -brane(s) ($p = 3, 5, 7$) into the gravity dual above. The action of a Dp -brane is the sum of the DBI and CS actions and takes the general form:

$$S_{Dp} = -g_s T_p \int d^{p+1} \xi e^{-\Phi} \sqrt{-\det(\gamma_{ab} + \mathcal{F}_{ab})} + g_s T_p \int \sum_p C_{p+1} \wedge e^{\mathcal{F}_{ab}}. \quad (2.6)$$

Here C_{p+1} are the IIB R–R background fields coupling to the Dp -brane world volume; $\mathcal{F}_{ab} = \mathcal{B}_{ab} + 2\pi\alpha' F_{ab}$ is the gauge invariant field strength with F_2 the world volume gauge field and \mathcal{B}_2 the pullback of the NS–NS two-form background field, B_2 , onto the world volume, $\mathcal{B}_{ab} = B_{MN}\partial_a X^M \partial_b X^N$, $\gamma_{ab} = g_{MN}\partial_a X^M \partial_b X^N$ the pullback of the ten-dimensional metric g_{MN} in string frame, and $\Phi = 0$. Lastly, ξ^a denote the world volume coordinates and $T_p = [(2\pi)^p g_s(\alpha')^{(p+1)/2}]^{-1}$ is the Dp -brane tension.

In what follows, we first consider the KW gravity dual described with metric (2.5) and write down the explicit form of the probe Dp -brane ($p = 3, 5, 7$) actions, (2.6), and world volume fields in the U-like embeddings of BKS models. We then modify the BKS models by turning on angular motion and world volume fields, and compute the induced world volume metrics and Hawking temperatures on the rotating probes.

2.2 U-like embedded probe D7-branes wrapping $adS_5 \times S^3 \subset adS_5 \times T^{1,1}$

As first example, we consider the U-like brane embedding configuration of ref. [21], embedding U-like probe D7-branes into the KW gravity dual, corresponding to adding flavored quarks to its dual gauge theory with spontaneous breakdown of the conformal and chiral flavor symmetry. In the KW gravity dual, the probe D7-brane wraps the entire dual spacetime coordinates $\{t, x_i, r\}$ ($i = 1, 2, 3$) of adS_5 in the 01234-directions, and the three-sphere $S^3 \subset T^{1,1}$ parameterized by the forms $\{\Omega_i\}$ in the 567-directions. Therefore the transverse space is given by the two-sphere $S^2 \subset T^{1,1}$ parameterized by the coordinates θ and ϕ in the 89-directions. This all can be summarized and represented by the array:

$$\begin{array}{cccccccccc} 0 & 1 & 2 & 3 & 4 & 5 & 6 & 7 & 8 & 9 \\ D3 & \times & \times & \times & \times & & & & & \\ D7 & \times & \times & \times & \times & \times & \times & \times & \times & \times \end{array}$$

Here we note that, as w_i are left-invariant forms, the ansatz preserves one of the $SU(2)$ factors of the global symmetry group of the conifold, $SU(2) \times SU(2) \times U(1)$. Thus, one may assume that the coordinates θ and ϕ are independent of the S^3 coordinates. The embedding breaks one of $SU(2)$, but by expanding the action around the solution it can be shown that contribution from the nontrivial S^3 show up only at the second order fluctuations. Thus, one can assume, in classical sense, that θ and ϕ depend only on the radial coordinate, r , of the conifold geometry.

The Kuperstein–Sonnenschein embedding of the D7-branes includes two choices. There is one choice where the D7-branes are placed on two separate points of the S^2 , with both of them stretched down to the tip of the conifold at $r = 0$ where both the S^2 and S^3 shrink to zero size. The configuration produced, in this case, is V -like. There is another choice where the D7-branes are placed on the S^2 with both of them smoothly merged into a single stack somewhere at $r = r_0$ above the conifold tip point. The configuration produced, in this case, is U -like. In both of the

U -like and V -like configurations, the D7-brane(s) wrap the $adS_5 \times S^3$ spacetime, as in the array above. However, on the transversal S^2 , here are two different pictures. In the V -like configuration, the D7-branes look like two separate fixed points while the U -like configuration results an arc along the equator. The position of the two points, setting the position of the D7-branes, depends on r and with them smoothly connected in the midpoint arc at $r = r_0$. In the gravity dual, this configuration produces a one-parameter family of D-brane profiles with the parameter r_0 setting the minimal radial extension of the D7-brane.

By the choice of the world volume fields $\phi = \phi(r)$ and $\theta = \theta(r)$, it is easy to derive the induced world volume metric from (2.5) in terms of (2.4) and obtain from (2.6) the action of the form:

$$S_{D7} = -\tilde{T}_{D7} \int dr dt r^3 \sqrt{1 + \frac{r^2}{6}(\theta'^2 + \sin^2 \theta \phi'^2)}, \quad (2.7)$$

where $\tilde{T}_{D7} = N_f V_{\mathbb{R}^3} V_{S^3} T_{D7}$ with $T_{D7} = 1/(2\pi)^7 g_s(\alpha')^4$. The Lagrangian in (2.7) is $SU(2)$ invariant and therefore one can restrict motion to the equator of the S^2 parameterized by ϕ and $\theta = \pi/2$. In writing down the action (2.7) from (2.6), one has set $F_{ab} = 0$ and noted that since the KW gravity dual contains only R-R four-form fluxes, so there is no contribution from the CS part and therefore the D7-brane action is just the DBI action.

The solution of the equation of motion from the action (2.7) yields a one-parameter family of D7-brane profiles of the form:

$$\phi(r) = \sqrt{6} r_0^4 \int_{r_0}^r \frac{dr}{r \sqrt{r^8 - r_0^8}} = \frac{\sqrt{6}}{4} \cos^{-1} \left(\frac{r_0}{r} \right)^4. \quad (2.8)$$

The solution (2.8) describes two separate branches, a disconnected D7 and an anti D7-brane pair, including the V -like configuration, when $r_0 = 0$. On contrary, the solution (2.8) describes a single branch, including the U -like configuration, when the two branches merge at $r = r_0 > 0$. Furthermore, when the configuration is U -like, taking the limit $r \rightarrow r_0$ implies $\phi'(r) \rightarrow \infty$.

The solution (2.8) contains several important features. First, when the configuration is V -like, it is clear from $d\theta = d\phi = 0$ that the induced world volume metric is that of $adS_5 \times S^3$ and the configuration describes the conformal and chiral symmetric phase. On contrary, when the configuration is U -like, the induced world volume metric has no adS factor and the conformal and chiral flavor symmetry of the dual gauge theory must be broken spontaneously. Second, by taking the asymptotic UV limit, $r \rightarrow \infty$, (2.8) describes two constant solutions $\phi_{\pm} = \pm\sqrt{6}\pi/8$. This gives an asymptotic UV separation between the branes as $\Delta\phi = \phi_+ - \phi_- = \sqrt{6}\pi/4$, and an asymptotic expansion as $\phi \simeq \pm\sqrt{6}\pi/8 \pm \frac{\sqrt{6}}{4} (r_0/r)^4 + \dots$. The asymptotic UV

separation between the branes is r_0 independent. In the dual gauge field theory r_0 corresponds to a normalizable mode, a vacuum expectation value (VEV). The fact that r_0 is a modulus, or a flat direction, implies the spontaneous breaking of the conformal symmetry. The expansion reveals that a $\Delta = 4$ marginal operator has a VEV fixed by r_0 as $\langle O \rangle \sim r_0^4/(\alpha')^2$, the fluctuations of which gives the Goldstone boson associated with the conformal symmetry breakdown. Third, the solutions ϕ_{\pm} , giving an r_0 -independent UV separation, make the brane anti-brane interpretation natural. This is because the brane world volume admits two opposite orientations once the asymptotic points ϕ_{\pm} are approached. Fourth, the presence of both the D7 and anti D7-brane guarantees tadpole cancellation and annihilation of total charge on the transverse S^2 , and it breaks supersymmetry explicitly with the embedding being non-holomorphic.

To this end, one also notes that the above setup cannot be embedded in the $adS_5 \times S^5$ solution. This because the S^5 contains no nontrivial cycle and therefore the D7-brane will shrink to a point on the S^5 . This problem may be fixed by a specific choice of boundary conditions at infinity, but this turns out to be incompatible with the U -shape configuration of interest. In addition, tadpole cancellation by an anti-D7-brane is not required, since one has no 2-cycle as in the conifold framework.

2.3 U-like embedded probe D5-branes wrapping $adS_3 \times S^3 \subset adS_5 \times T^{1,1}$

As second example, we consider the U-like brane embedding configuration of ref. [28], embedding U-like probe D5-branes into the KW gravity dual, corresponding to adding defect flavored quarks to its dual gauge theory with spontaneous breakdown of the conformal and chiral flavor symmetry. In the KW gravity dual, the probe D5-brane wraps some of the dual spacetime coordinates, including $adS_3 \subset adS_5$, given by $\{t, x_i, r\}$ ($i = 1$) in the 014-directions, and the three-sphere $S^3 \subset T^{1,1}$ parameterized by the forms $\{\Omega_i\}$ in the 567-directions. Thus, in this example, the probe D5-brane wraps the $adS_3 \times S^3$ spacetime and the transverse space is given by the two-sphere $S^2 \subset T^{1,1}$ parameterized by the coordinates θ and ϕ in the 89-directions. This all can be summarized and represented by the array:

$$\begin{array}{cccccccccc} 0 & 1 & 2 & 3 & 4 & 5 & 6 & 7 & 8 & 9 \\ \text{D3} & \times & \times & \times & \times & & & & & \\ \text{D5} & \times & \times & & & \times & \times & \times & \times & \end{array}$$

By the choice of the world volume fields similar to the D7-brane above, $\phi = \phi(r)$ and $\theta = \text{const.}$, it is easy to derive the induced world volume metric from (2.5) in terms of (2.4) and obtain from (2.6) the action of the form:

$$S_{D5} = -\tilde{T}_{D5} \int dr dt r \sqrt{1 + \frac{r^2}{6} \phi'^2}, \quad (2.9)$$

where $\tilde{T}_{D5} \equiv N_f V_{\mathbb{S}^3} T_{D5}$. Here we note that the probe D5-brane wraps the same S^3 as the probe D7-brane above and the Lagrangian density in (2.9) is the same as the Lagrangian density in (2.7) modulo r^2 .

The solution of the equation of motion from the action (2.9) yields a one-parameter family of D5-brane profiles of the form:

$$\phi(r) = \frac{\sqrt{6}}{2} \left(\pm \frac{\pi}{2} \mp \arctan \left(\frac{r_0^2}{\sqrt{r^4 - r_0^4}} \right) \right). \quad (2.10)$$

The solution (2.10) has the same general features, and satisfies the same boundary conditions, as before. However, in this example, the UV separation is $\Delta\phi = \sqrt{6}\pi/2$, instead of $\Delta\phi = \sqrt{6}\pi/4$, in the previous example. Thus (2.10) represents another U-shape solution, though this time, dual to dCFT, with the additional quark fields residing in just two out of the four spacetime dimensions. The expected near boundary behavior of (2.10) is that of a VEV deformation of a marginal ($\Delta = 2$) operator in one dimension.

2.4 U-like embedded probe D5-branes wrapping $adS_4 \times S^2 \subset adS_5 \times T^{1,1}$

As third example, we consider the U-like brane embedding configuration of ref. [28], embedding U-like probe D5-branes alternatively, [34, 35], into the KW gravity dual, corresponding to adding defect flavored quarks to its dual gauge theory with spontaneous breakdown of the conformal and chiral flavor symmetry. In the KW gravity dual, the probe D5-brane wraps some of the dual spacetime coordinates, including $adS_4 \subset adS_5$, given by $\{t, x_i, r\}$ ($i = 1, 2$) in the 0124-directions, and the two-sphere $S^2 \subset T^{1,1}$ parameterized by θ_1, ϕ_1 in the 56-directions. Thus, in this example, the probe D5-brane wraps the $adS_4 \times S^2$ spacetime and the transverse space is given by the three-sphere $S^3 \subset T^{1,1}$ parameterized by the coordinates θ_2, ϕ_2 and ψ in the 789-directions. This all can be summarized and represented by the array:

$$\begin{array}{cccccccccc} 0 & 1 & 2 & 3 & 4 & 5 & 6 & 7 & 8 & 9 \\ \text{D3} & \times & \times & \times & \times & & & & & \\ \text{D5} & \times & \times & \times & & \times & \times & \times & & \end{array}$$

By the choice of the world volume fields $\theta_2 = \pi - \theta_1$, $\phi_1 = \phi_2$, and $\psi = \psi(r)$ it is easy to derive the induced world volume metric from the metric (2.5) in terms of (2.3) and obtain from (2.6) the action of the form:

$$S_{D5} = -\tilde{T}_{D5} \int dr dt r^2 \sqrt{1 + \frac{r^2}{9} \psi'^2}, \quad (2.11)$$

where $\tilde{T}_{D5} \equiv N_f V_{\mathbb{S}^2} T_{D5}$. Here we note that the probe D5-brane wraps this time the S^2 , unlike in the previous example, and the Lagrangian density in (2.11) is not the same as the Lagrangian density in (2.9).

The solution of the equation of motion from the action (2.11) yields a one-parameter family of D5-brane profiles of the form:

$$\psi(r) = \pm \frac{\pi}{2} \mp \arcsin \left(\frac{r_0^3}{r^3} \right). \quad (2.12)$$

The solution (2.12) has the same of the general features, and meets the same boundary conditions, as before. However, in this example, the UV separation is given by $\Delta\psi = \psi_+ - \psi_- = \pi/2 - (-\pi/2) = \pi$, with both ψ_{\pm} corresponding to supersymmetric D5-brane embedding and preserving different supersymmetries. Thus (2.12) represents another U-shape solution, though this time, supersymmetric and dual to dCFT, with the additional quark fields residing in three out of the four spacetime dimensions. The expected near boundary behavior of (2.12) is that of a VEV deformation of a marginal $\Delta = 2$ operator.

2.5 U-like embedded probe D3-branes wrapping $adS_2 \times S^2 \subset adS_5 \times T^{1,1}$

As final example, we consider the U-like brane embedding configuration of ref. [28], embedding U-like probe D3-branes into the KW gravity dual, corresponding to adding defect flavored quarks to its dual gauge theory with spontaneous breakdown of the conformal and chiral flavor symmetry. In the KW gravity dual, the probe D3-brane wraps some of the dual spacetime coordinates, including $adS_2 \subset adS_5$, given by $\{t, r\}$ in the 04-directions, and the two-sphere $S^2 \subset T^{1,1}$ parameterized by θ_1, ϕ_1 in the 56-directions. Thus, the probe D3-brane wraps the $adS_2 \times S^2$ spacetime and the transverse space is given by the three-sphere $S^3 \subset T^{1,1}$ parameterized by the coordinates θ_2, ϕ_2 and ψ in the 789-directions. This all can be summarized and represented by the array:

$$\begin{array}{cccccccccc} 0 & 1 & 2 & 3 & 4 & 5 & 6 & 7 & 8 & 9 \\ \text{D3} & \times & \times & \times & \times & & & & & \\ \text{D3} & \times & & & & & \times & \times & \times & \end{array}$$

By the choice of the world volume fields similar to the probe D5-brane above, $\phi = \theta = \text{const.}$ and $\psi = \psi(r)$, it is easy to derive the induced world volume metric from (2.5) in terms of (2.3) and obtain from (2.6) the action of the form:

$$S_{D3} = -\tilde{T}_{D3} \int dr dt \sqrt{1 + \frac{r^2(\psi')^2}{9}}, \quad (2.13)$$

where $\tilde{T}_{D3} = N_f V_{S^2} T_{D3}$. We also note that the Lagrangian density in (2.13) is, up to a radial factor, r^2 , the same as the density of the probe D5-brane in (2.11).

The solution of the equation of motion from the action (2.13) yields a one-parameter family of D3-brane profiles of the form:

$$\psi(r) = \mp \frac{3\pi}{2} \pm 3 \arctan \left(\frac{r_0}{\sqrt{r^2 - r_0^2}} \right). \quad (2.14)$$

The solution (2.14) has the same general features, and satisfies the same boundary conditions, as before. However, in this example, the UV separation is $\Delta\psi = 3\pi$ whereby the brane never wraps the internal cycle more than once, as $\psi \in [0, 4\pi]$. Thus (2.14) represents another U-shape solution dual to dCFT, with the additional quark fields being “quantum mechanical”, – depending only on time and not on space. The expected near boundary behavior of (2.14) is that of a VEV deformation of a marginal ($\Delta = 1$) operator in one dimension.

3. Induced metric and temperature on U-like embedded probe D7-brane wrapping $adS_5 \times S^3 \subset adS_5 \times T^{1,1}$ and spinning about $S^2 \subset T^{1,1}$ with world volume electric field turned on

As first example in our study, we consider the U-like probe D7-brane model wrapping $adS_5 \times S^3$ in $adS_5 \times T^{1,1}$ reviewed in Sec. 2, and turn on, in addition, spin as well as world-volume gauge electric field on the probe, following closely [20]. We include additional spin degrees of freedom, dual to finite R-charge chemical potential, by allowing in our system the D7-brane rotate in the ϕ direction of the transverse S^2 with conserved angular momentum. Thus, in our setup, we allow ϕ to have time-dependence as well, such that $\dot{\phi}(r, t) = \omega = const.$, with ω denoting the angular velocity of the probe. This way, we construct rotating solutions. Hence, the world-volume field is given by $\phi(r, t)$, with other directions fixed. We also include the additional contribution from world-volume fields strengths, F_{ab} , in (2.6), corresponding to world-volume gauge fields, dual to finite baryon density chemical potential, by noting the following: In the presence of N_f flavors, the gauge theory posses a global $U(N_f) \simeq SU(N_c) \times U(1)_q$ symmetry. The $U(1)_q$ counts the net number of quarks, that is, the number of baryons times N_c . In the gravity dual, this global symmetry corresponds to the $U(N_f)$ gauge symmetry on the world volume of the N_f D7-brane probes. The conserved currents associated with the $U(N_f)$ symmetry of the gauge theory are dual to the gauge fields, A_μ , on the D7-branes. Hence the introduction of a chemical potential μ or a non-vanishing n_B for the baryon number the gauge theory corresponds to turning on the diagonal $U(1) \subset U(N_f)$ gauge field, A_μ on the world volume of the D7-branes. We may describe external fields in the field theory, coupled to anything having $U(1)$ charge, by introducing non-normalizable modes for A_μ in the gravity dual (e.g. see ref. [6, 9]).

In this section therefore we will study U-like embedded probe D7-branes spinning with an angular frequency ω , and with a $U(1)$ world volume gauge field A_μ . We

note that in order to have the gauge theory at finite chemical potential or baryon number density, it suffices to turn on the time component of the gauge field, A_t . By symmetry considerations, one may take $A_t = A_t(r)$. As we shall briefly discuss below, a potential of this form will support an electric field.

Therefore, we will consider the ansatz for the D7-brane world-volume field of the form $\phi(r, t) = \omega t + f(r)$, with other directions fixed, and $F_{ab} = F_{rt} = \partial_r A_t(r)$. Using this ansatz and the metric (2.5) in terms of (2.4), it is easy to derive the components of the induced world-volume metric on the D7-brane, g_{ab}^{D7} , and compute the determinant, $\det g_{ab}^{D7}$, resulting the DBI action (2.6), as:

$$S_{D7} = -\tilde{T}_{D7} \int dr dt r^3 \sqrt{1 - \frac{L^4 \dot{\phi}^2}{6r^2} + \frac{r^2 (\phi')^2}{6} - (A'_t(r))^2}. \quad (3.1)$$

Here we note that by setting $\dot{\phi} = \omega = A_t(r) = 0$, our action (3.1) reduces to that of the probe D7-brane action in the Kuperstein–Sonnenschein model, (2.7). As in the Kuperstein–Sonnenschein model reviewed in Sec. 2, we restrict brane motion to the ϕ -direction of the transverse S^2 sphere and fix other directions constant. Thus, in our set-up we let, in addition, the probe rotate about the S^2 , and furthermore turn on a non-constant world-volume electric on the probe.

The D7-brane equations of motion from the action (3.1) read:

$$\frac{\partial}{\partial r} \left[\frac{r^5 \phi'}{\sqrt{1 + \frac{r^2 (\phi')^2}{6} - \frac{L^4 \dot{\phi}^2}{6r^2} - (A'_t(r))^2}} \right] = \frac{\partial}{\partial t} \left[\frac{L^4 r \dot{\phi}}{\sqrt{1 + \frac{r^2 (\phi')^2}{6} - \frac{L^4 \dot{\phi}^2}{6r^2} - (A'_t(r))^2}} \right], \quad (3.2)$$

$$\frac{\partial}{\partial r} \left[\frac{r^3 A'_t(r)}{\sqrt{1 + \frac{r^2 (\phi')^2}{6} - \frac{L^4 \dot{\phi}^2}{6r^2} - (A'_t(r))^2}} \right] = 0. \quad (3.3)$$

By taking the large radii limit, $r \rightarrow \infty$, it is straightforward to see that Eq. (3.3) solves to $A_t(r) \simeq \mu - a_B/r^2$, with μ being the chemical potential and a_B the VEV of baryon density number. We note that this solution for A_t is of expected form, since an electric field will be supported by a potential of the form $A_t \simeq r^{-2}$. Since this is a rank one massless field in adS , it must correspond to a dimension four operator or current in the gauge theory. This is just what one would expect from an R-current, to which gauge fields correspond.

Take rotating solutions to (3.2) of the form:

$$\phi(r, t) = \omega t + f(r), \quad f(r) = \sqrt{6} r_0^4 \int_{r_0}^r \frac{dr}{r} \sqrt{\frac{1 - L^4 \bar{\omega}^2 / r^2 - (A'_t(r))^2}{r^8 - r_0^8}}. \quad (3.4)$$

Here we set $\bar{\omega} = \omega/\sqrt{6}$ and note that when $\omega = A_t(r) = 0$, our solution (3.4) integrates to that of probe D7-brane in the Kuperstein–Sonnenschein model, [21], reviewed in Sec. 2, with the probe wrapping $adS_3 \times S^3$ in $adS_5 \times T^{1,1}$ (see Eq. (2.8)). The solution (3.4) is parameterized by (r_0, ω, a_B) and describes probe D7-brane motion, with non-constant world-volume gauge field $A_t(r)$ and angular velocity ω about the transverse $S^2 \subset T^{1,1}$, starting and ending up at the boundary. The probe descends from the UV boundary at infinity to the minimal extension r_0 in the IR where it bends back up the boundary. We also note that inspection of (3.4) illustrates, in the limit $r \rightarrow \text{large}$, that the behavior of $df(r)/dr = f_r(r)$ does not depend on ω and a_B (see Fig. 1). This illustrates that in the large radii limit the solution $f(r)$ in (3.4) gives the world-volume field $\phi(r)$ of the Kuperstein–Sonnenschein model (see Sec. 2) with the boundary values ϕ_{\pm} in the asymptotic UV limit, $r \rightarrow \infty$ (see also Fig. 1). But, we note that in the (other) IR limit, i.e., when $r \rightarrow \text{small}$, the behavior of $f_r(r)$ does depend on ω . Furthermore, we note here that by turning on, in addition, the world volume electric field merely changes the scale but leaves the behavior of $f_r(r)$ in the IR unchanged. Inspection of (3.4) illustrates that in the IR the behavior of $f_r(r)$ with $\omega > 0$ is comparable to that of with $\omega = 0$, only if certain $\omega > 0$ are chosen (see Fig. 1). This illustrates that in the small radii limit in the IR the behavior of $f_r(r)$ (here) does compare to that of $\phi'(r) = d\phi/dr$ in the Kuperstein–Sonnenschein model (see Sec. 2),—with $\phi'(r) \rightarrow \infty$ in the IR limit $r \rightarrow r_0^-$, consistent with U-like embedding, only if certain $\omega > 0$ are chosen.

To derive the induced metric on the D5-brane, we put the rotating solution (3.4) into the background metric (2.5) in terms of (2.4) and obtain:

$$\begin{aligned}
ds_{D7}^2 = & -\frac{1}{3L^2}(3r^2 - L^4\omega^2)dt^2 \\
& + \frac{L^2}{r^2} \left[\frac{3r^2(r^8 - r_0^8) + r_0^8(6r^2(1 - (A'_t(r))^2) - L^4\omega^2)}{3r^2(r^8 - r_0^8)} \right] dr^2 \\
& + \frac{2L^2\omega r_0^4}{3r^2} \sqrt{\frac{6r^2(1 - (A'_t(r))^2) - L^4\omega^2}{r^8 - r_0^8}} dr dt \\
& + \frac{r^2}{L^2}(dx^2 + dy^2 + dz^2) + \frac{L^2}{3} \left[\frac{1}{2}(\Omega_1^2 + \Omega_2^2) + \frac{1}{3}\Omega_3^2 \right] \\
& - \frac{L^2}{3} \left[\omega\Omega_1 dt + \frac{r_0^4}{r^2} \sqrt{\frac{6r^2(1 - (A'_t(r))^2) - L^4\omega^2}{r^8 - r_0^8}} \Omega_1 dr \right]. \tag{3.5}
\end{aligned}$$

Here we note that by setting $\omega = A_t = 0$, our induced world-volume metric (3.5) reduces to that of the Kuperstein–Sonnenschein model, [21], reviewed in Sec. 2. In this case, for $r_0 = 0$ the induced world-volume metric is that of $adS_5 \times S^3$ and the dual gauge theory describes the conformal and chiral symmetric phase. On contrary, for $r_0 > 0$ the induced world volume metric has no adS factor and the conformal

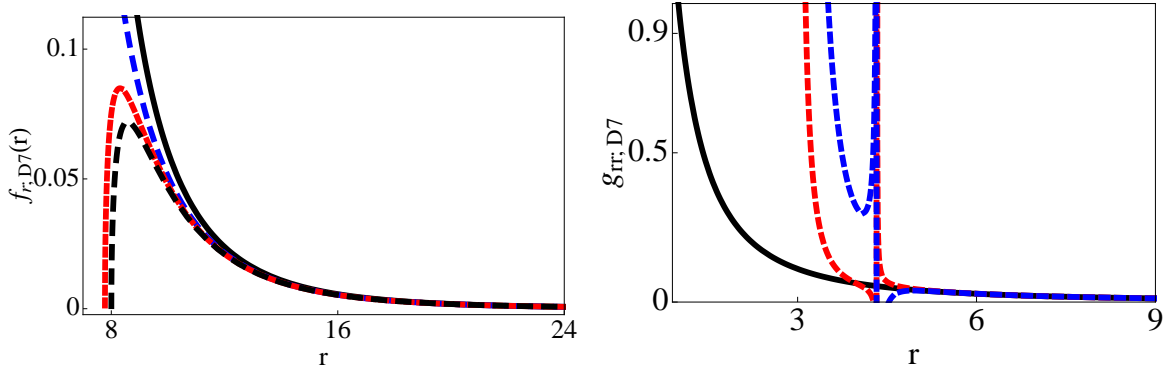


Figure 1: [Left] The behavior of the derivative of the world volume field with respect to r with $L = 1, r_0 = 7, \omega = 0, a_B = 0$ (black-solid), $\omega = 7.5, a_B = 100$ (blue-dashed), $a_B = 180$ (red-dashed), and $a_B = 200$ (black-dashed). [Right] The behavior of the g_{rr} component of the induced world volume metric with $L = 1, r_0 = \omega = a_B = 0$ (black-solid), $r_0 = 3, \omega = 7.5, a_B = 20$ (red-dashed), and $a_B = 60$ (blue-dashed).

invariance of the dual gauge theory must be broken in such case. In order to find the world-volume horizon and Hawking temperature, we first eliminate the relevant cross term. To eliminate the relevant cross-term in (3.5), we consider a coordinate transformation:

$$\tau = t - \omega L^4 r_0^4 \int \frac{dr (6r^2(1 - (A'_t(r))^2) - L^4 \omega^2)^{1/2}}{r^2(3r^2 - L^4 \omega^2)(r^8 - r_0^8)^{1/2}}. \quad (3.6)$$

The induced metric on the rotating D7-brane(s) then takes the form:

$$\begin{aligned} ds_{D7}^2 = & -\frac{(3r^2 - L^4 \omega^2)}{3L^2} d\tau^2 \\ & + \frac{L^2}{r^2} \left[\frac{(3r^2 - L^4 \omega^2)(r^8 - r_0^8) + r_0^8(6r^2(1 - (A'_t(r))^2) - L^4 \omega^2)}{(3r^2 - L^4 \omega^2)(r^8 - r_0^8)} \right] dr^2 \\ & + \frac{r^2}{L^2} (dx^2 + dy^2 + dz^2) + \frac{L^2}{3} \left[\frac{1}{2}(\Omega_1^2 + \Omega_2^2) + \frac{1}{3}\Omega_3^2 \right] \\ & - \frac{L^2}{3} \left[\omega \Omega_1 d\tau + \frac{3r_0^4}{3r^2 - L^4 \omega^2} \sqrt{\frac{6r^2(1 - (A'_t(r))^2) - L^4 \omega^2}{r^8 - r_0^8}} \Omega_1 dr \right]. \quad (3.7) \end{aligned}$$

Here we note that for $r_0 = 0$ the induced world-volume metric (3.7) has no horizon solving $-g_{\tau\tau} = g^{rr} = 0$, and thus not given by the black hole geometry. On contrary, for $r_0 > 0$ the induced world-volume horizon solves the equation:

$$H(r) = r^2(r^8 - r_0^8)(3r^2 - L^4 \omega^2) = 0. \quad (3.8)$$

Eq.(3.8) contains two real positive definite zeros (see also Fig.1). The thermal horizon of the induced world-volume black hole geometry is given by the zero $3r_H^2 -$

$L^4\omega^2 = 0$, with the horizon varying continuously with varying the angular velocity ω , as expected. Eq. (3.8) also shows that the horizon must grow from the minimal extension $r_0 \neq 0$ with increasing the angular velocity ω . We thus conclude at this point that when r_0 is positive definite ($r_0 > 0$) and spin is turned on ($\omega > 0$), the induced world-volume metric on the rotating probe D7-brane wrapping $adS_5 \times S^3$ in $adS_5 \times T^{1,1}$ admits a thermal horizon growing continuously with increasing the angular velocity, regardless of the presence of the world-volume gauge electric field.

The Hawking temperature on the probe D7-brane can be found from the induced world-volume metric (3.7) in the form:

$$T_{H;D7} = \frac{(g^{rr})'}{4\pi} \Big|_{r=r_H} = \frac{3r_H^3(r_H^8 - r_0^8)}{2\pi L^2 r_0^8 [6r_H^2(1 - (A'_t(r))^2) - L^4\omega^2]} = \frac{r_H^7(r_H^8 - r_0^8)}{2\pi L^2 r_0^8 (r_H^6 - 8a_B^2)}. \quad (3.9)$$

Here, we note from (3.9) that when the world volume horizon is at the minimal radial extension, $r_H = r_0$, the Hawking temperature of the world volume black hole geometry is identically zero, $T_{H;D7} = 0$. The Hawking temperature (3.9) of the world-volume black hole solution (3.7) also has a number of interesting features, which depend on the choice of parameters $\{a_B, r_0, \omega\}$. Thus we note the following points:

- For $a_B = 0$, $r_0 = 4$ and $\omega \geq 0$, the world-volume Hawking temperature $T_{H;D7}$ (3.9) increases monotonically with increasing the angular velocity ω , by which the world volume horizon size r_H grows (see Fig. 2). In this case, changing r_0 changes the scale, but not the behavior of the temperature (3.9). In particular, inspection of (3.9) shows that decreasing/increasing r_0 increases/decreases the temperature and produces a large hierarchy between temperature scales, $T_{H;D7}(r_0 < 1)/T_{H;D7}(r_0 > 1) \simeq 10^8$, while the temperature behavior remains unchanged (see Fig. 2).
- For $0 < a_B \leq 180$, $r_0 = 4$ and $\omega \geq 0$, the world-volume Hawking temperature $T_{H;D7}$ (3.9) no longer behaves monotonically with growing the horizon size r_H . Instead, the temperature of the solution (3.9) admits three distinct branches, including two obvious classes of black hole solutions (see Fig. 2). The first branch appears once the horizon starts to grow from the minimal extension r_0 . In this case, the temperature $T_{H;D7}$ (3.9) decreases almost immediately to negative values⁸, before peeking off very sharply, whereby producing a divergent-like behavior, hitting zero, and then growing into positive values (see Fig. 2). The second branch appears once the horizon continues to grow, away from the zero point. In this case, the temperature $T_{H;D7}$ (3.9) decreases to positive values, in an ‘inverse-like’ manner with the horizon, before reaching its non-zero minimum (see Fig. 2). Therefore in the neighborhood of the

⁸Here we note that in other interesting study in the literature, ref. [33], using similar D-brane systems, it has been shown that when just an electric field is turned on (in place of rotation, or R-charge, considered here), in certain codimensions, the induced world-volume temperature of the probe is given by a decreasing function of the electric field (see Eq. (24) in ref. [33])

zero point the world-volume temperature of the solution decreases with increasing horizon size. These ‘small’ black holes have the familiar behavior of five-dimensional black holes in asymptotically flat spacetime, since their temperature decreases with increasing horizon size r_H . The third branch appears once the horizon continues to grow from its radius setting the non-zero minimum of $T_{H;D7}$. In this case, the other class of black hole solution appears with its temperature only increasing with increasing horizon size r_H , like ‘large’ black holes (see Fig. 2). This behavior is like that of the temperature with $a_B = 0$, however, in the latter two branches, the temperature of the black hole solution scales higher than that of with $a_B = 0$ (see Fig. 2). It is thus remarkable that by varying a_B , the scale and behavior of the temperature changes continuously with growing horizon size r_H (see Fig. 2). It is clear that by increasing/decreasing a_B the temperature behavior changes dramatically, while the temperature scales change very moderately, producing only small hierarchies, $T_{H;D7}(a_B <)/T_{H;D7}(a_B >) \simeq 0.5$ (see Fig. 2).

- By varying r_0 , while keeping the other parameters within the above range, the scale and behavior of the temperature of the black hole solution, $T_{H;D7}$ (3.9), change dramatically once again. For $r_0 < 1$, only the temperature scale changes, but for $r_0 > 1$, i.e., $r_0 \simeq 8$, the scale and, in particular, the behavior of the temperature change dramatically. In this latter case, the temperature scales much less than in previous cases ($r_0 > 1$), increases with increasing a_B as before, and behaves similarly to the temperature with $a_B = 0$, increasing continuously with growing r_H , despite now $a_B \neq 0$ (see Fig. 2). In this latter case, therefore there is only one branch, corresponding to one class of black hole solution, including ‘large’ black holes only, with temperature scales setting relatively large hierarchies, $T_{H;D7}(r_0 <)/T_{H;D7}(r_0 >) \simeq 10^3$.

We therefore conclude at this point that when the minimal extension changes, the temperature scale of the world volume black hole solution changes dramatically and sets large hierarchies, while the temperature behavior remains unchanged. We conclude, however, that when the world volume electric field is turned on, the temperature behavior changes dramatically and includes two distinct branches corresponding to ‘large’ and ‘small’ black hole solutions, respectively, while the temperature scale changes moderately and thereby sets only moderate hierarchies. In this case, we conclude, however, that when, in addition, the minimal extension gets increased, the temperature behavior changes once again dramatically and includes only one branch corresponding to ‘large’ black holes, with the temperature scale setting relatively large hierarchies.

We further notice that by taking into account the backreaction of the above solution to the KW gravity dual, $adS_5 \times T^{1,1}$, one accordingly awaits the D7-brane to form a mini black hole in KW, corresponding to a locally thermal gauge field theory in the probe limit. Thereby, the rotating D7-brane describes a thermal object in the dual gauge field theory. In the KW example here, the configuration is dual to $\mathcal{N} = 1$ gauge theory coupled to a flavor subject to an external electric field. As the gauge

theory itself is at zero temperature, while its flavor sector is at finite temperature, given by (3.9), we conclude that the configuration describes non-equilibrium steady state. However, as we shall show below, the energy from the flavor sector will in the end dissipate into the gauge theory conformal and chiral flavor symmetry breakdown.

So far, in this example, we neglected the backreaction of the D7-brane to the KW gravity dual, as we worked in the probe limit. It is useful to observe the extend this is justifiable. To this end, we derive the components of the energy–stress tensor of the rotating D7-brane, which take the form:

$$\begin{aligned}\sqrt{-g}J_{t;D7}^t &\equiv \frac{\tilde{T}_{D7} r^3 (1 + r^2 (\phi')^2 / 6)}{\sqrt{1 + r^2 (\phi')^2 / 6 - L^4 \dot{\phi}^2 / 6r^2 - (A')^2}} \\ &= \frac{\tilde{T}_{D7} (r^4 (r^{10} - L^4 \bar{\omega}^2 r_0^8) - 4r_0^8 a_B^2)}{r^4 \sqrt{(r^8 - r_0^8)(r^6 - L^4 \bar{\omega}^2 r^4 - 4a_B^2)}},\end{aligned}\quad (3.10)$$

$$\begin{aligned}\sqrt{-g}J_{r;D7}^r &\equiv -\frac{\tilde{T}_{D7} r^3 (1 - L^4 \dot{\phi}^2 / 6r^2)}{\sqrt{1 + r^2 (\phi')^2 / 6 - L^4 \dot{\phi}^2 / 6r^2 - (A')^2}} \\ &= -\tilde{T}_{D7} (r^2 - L^4 \bar{\omega}^2) \sqrt{\frac{r^8 - r_0^8}{r^6 - L^4 \bar{\omega}^2 r^4 - 4a_B^2}},\end{aligned}\quad (3.11)$$

$$\sqrt{-g}J_{t;D7}^r \equiv \frac{\tilde{T}_{D7} r^5 \dot{\phi} \phi'}{\sqrt{1 + r^2 (\phi')^2 / 6 - L^4 \dot{\phi}^2 / 6r^2 - (A')^2}} = \tilde{T}_{D7} r_0^4 \omega. \quad (3.12)$$

Using (3.10)–(3.12), we can derive the total energy and energy flux of the D-brane system. The total energy of the D7-brane in the above configuration is given by:

$$E = \tilde{T}_{D7} \int_{r_0}^{\infty} \frac{dr (r^4 (r^{10} - L^4 \bar{\omega}^2 r_0^8) - 4r_0^8 a_B^2)}{r^4 \sqrt{(r^8 - r_0^8)(r^6 - L^4 \bar{\omega}^2 r^4 - 4a_B^2)}}. \quad (3.13)$$

It is straightforward to see from (3.13) that when $r \rightarrow r_0$, the energy density of the flavor brane, given by (3.10), becomes very large and blows up precisely at the minimal extension, $r = r_0$, at the IR scale of conformal and chiral flavor symmetry breakdown, independent from the presence of the world volume electric field. Thus we conclude that at the IR scale, $r = r_0$, the backreaction of the D7-brane to the gravity dual metric is non-negligibly large and forms a black hole centered at the IR scale $r = r_0$ in the bulk. The black hole size should grow as the energy gets pumped into it from the D7-brane steadily. In order to obtain this energy flux, we use the components of the energy–stress tensor (3.10)–(3.12). We note that when the minimal radial extension is positive definite ($r_0 > 0$) and spin is turned on ($\omega > 0$), the component (3.12) is non-vanishing and hence we compute the time evolution of

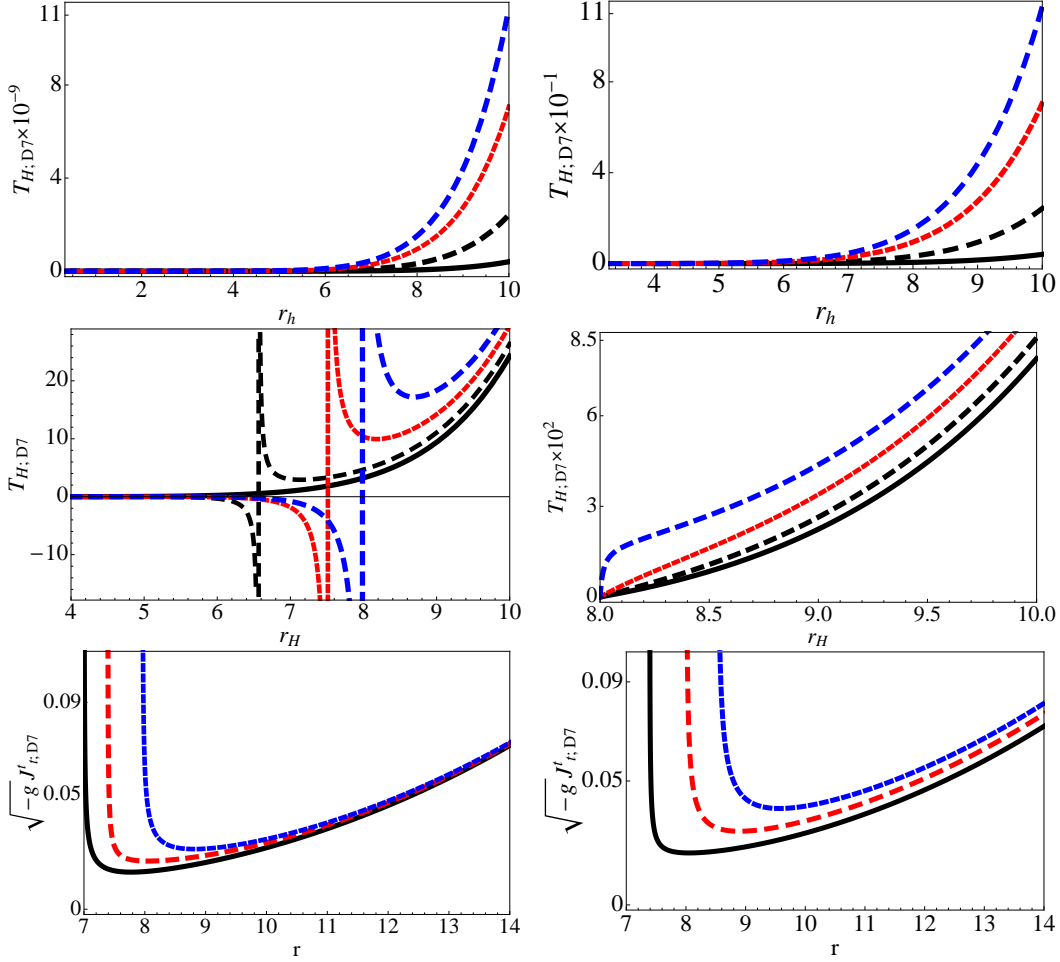


Figure 2: [Up-Left] The behavior of the world volume Hawking temperature with $r_0 = 5$ (solid), $r_0 = 4$ (black-dashed), $r_0 = 3.5$ (gray-dashed), $r_0 = 3.3$ (blue-dashed), and $L = 10$. [Up-Right] The behavior of the temperature with $r_0 = 0.5$ (black-solid), $r_0 = 0.4$ (black-dashed), $r_0 = 0.35$ (red-dashed), $r_0 = 0.33$ (blue-dashed), and $L = 10$. [Middle-Left] The behavior of the temperature in the presence of the world volume electric field with $a_B = 0$ (black-solid), $a_B = 100$ (black-dashed), $a_B = 150$ (red-dashed), $a_B = 180$ (blue-dashed), $r_0 = 4$, and $L = 10$. [Middle-Right] The behavior of the temperature in the presence of the world volume electric field with $a_B = 0$ (black-solid), $a_B = 100$ (black-dashed), $a_B = 150$ (red-dashed), $a_B = 180$ (blue-dashed), $r_0 = 8$, and $L = 10$. [Down-Left] The behavior of the energy-density, $\sqrt{-g} J^t_{t;D7}$, with $a_B = 0$ (black-solid), $a_B = 200$ (red-dashed) $a_B = 250$ (blue-dashed), and $r_0 = 7$ and $\omega = 1$. [Down-Right] The behavior of the energy-density with $\omega = 1$ (black-solid), $\omega = 5$ (red-dashed) $\omega = 6.5$ (blue-dashed), and $r_0 = 7$ and $a_B = 200$. In all cases, $L = \alpha' = 1$ and $g_s = 0.1$.

the total energy as:

$$\dot{E}_{D7} = \frac{d}{dt} \int dr \sqrt{-g} J^t_{t;D7} = \int dr \partial_r (\sqrt{-g} J^r_{t;D7}) = \sqrt{-g} J^r_{t;D7} \big|_{r=r_0}^\infty = \tilde{T}_{D7} r_0^4 \omega^2 - \tilde{T}_{D7} r_0^4 \omega^2 = 0. \quad (3.14)$$

Here we note that when the electric field is turned on, $J_{t,D7}^r$, given by (3.12), and the energy dissipation \dot{E}_{D7} , given by (3.14), remain unchanged. Therefore, independent from the electric field, the energy dissipation from the brane into the bulk will form a black hole, centered at the IR scale $r = r_0$. Thus, by this flow of energy from the probe to the bulk, we conclude by duality that the energy from the flavor sector will eventually dissipate into the gauge theory conformal and chiral flavor symmetry breakdown, independent from the electric field. To see this external injection of energy in our stationary rotating solution, we may introduce UV and IR cut offs to the D7-brane solution, such that it extends from $r = r_{\text{IR}} = r_0$ to $r = r_{\text{UV}} \gg r_{\text{IR}}$. It is clear from (3.12) that at both r_{IR} and $r = r_{\text{UV}}$ we have $J_t^r > 0$. This shows the presence of equal energy flux incoming from $r = r_{\text{UV}}$ and outgoing at $r = r_{\text{IR}}$ at which the energy gets not reflected back but its backreaction will nucleate a black hole intaking the injected energy, independent from the electric field.

The energy-density (3.10) of the world-volume black hole solution (3.7) has a number of interesting features. These depend on the choice of parameters $\{r_0, a_B, \omega\}$, and therefore we note the following points.

- Increasing ω , while keeping the other parameters fixed, increases the scale of the minimum energy-density near the IR scale, and also increases the amount of energy density away from the IR scale (see Fig. 2). However, the increase in the energy-density is so that the backreaction remains negligibly small away from the blowing up point, located at the IR scale r_0 (see Fig. 2).
- Increasing a_B by relatively large values, while keeping the other parameters fixed, only shifts the minimum of the energy-density and leaves the scale and behavior of the energy-density unaltered (see Fig. 2).
- Increasing/decreasing r_0 , while keeping the other parameters fixed, leaves the scale and behavior of the energy-density unaltered (as in Fig. 2).

In all cases, the energy-density falls sharply from its infinite value at the IR scale to its minimum value, whereupon it increases to finitely small values away from the IR scale. We thus conclude that altering the parameters of the solution results almost no alteration in the scale and behavior of the energy-density, meaning that the density blows up at the IR scale, whereat the backreaction is non-negligible, and stays finitely small away from the IR scale, where the backreaction can be neglected.

4. Induced metric and temperature on U-like embedded probe D5-brane wrapping $adS_3 \times S^3 \subset adS_5 \times T^{1,1}$ and spinning about $S^2 \subset T^{1,1}$ with world volume electric field turned on

As second example in our study, we consider the U-like probe D5-brane model wrapping $adS_3 \times S^3$ in $adS_5 \times T^{1,1}$ reviewed in Sec. 2, and turn on, in addition, spin as well as world-volume gauge electric field on the probe. We include additional spin degrees

of freedom, dual to finite R-charge chemical potential, by allowing in our system the D5-brane rotate in the ϕ direction of the transverse S^2 with conserved angular momentum. Thus, in our setup, we allow ϕ to have time-dependence as well, such that $\dot{\phi}(r, t) = \omega = \text{const.}$, with ω denoting the angular velocity of the probe. This way, we construct rotating solutions. Hence, the world-volume field is given by $\phi(r, t)$, with other directions fixed. We also include the additional contribution from world-volume fields strengths, F_{ab} , in (2.6), corresponding to world-volume gauge fields, dual to finite baryon density chemical potential, by noting the following: In the presence of N_f flavors, the gauge theory posses a global $U(N_f) \simeq SU(N_c) \times U(1)_q$ symmetry. The $U(1)_q$ counts the net number of quarks, that is, the number of baryons times N_c . In the gravity dual, this global symmetry corresponds to the $U(N_f)$ gauge symmetry on the world volume of the N_f D5-brane probes. The conserved currents associated with the $U(N_f)$ symmetry of the gauge theory are dual to the gauge fields, A_μ , on the D5-branes. Hence the introduction of a chemical potential μ or a non-vanishing n_B for the baryon number the gauge theory corresponds to turning on the diagonal $U(1) \subset U(N_f)$ gauge field, A_μ on the world volume of the D5-branes. We may describe external fields in the field theory, coupled to anything having $U(1)$ charge, by introducing non-normalizable modes for A_μ in the gravity dual (e.g. see ref. [6, 9]).

In this section, we will study U-like embedded probe D5-branes spinning with angular frequency ω , and with a $U(1)$ world volume gauge field A_μ . To have the gauge theory at finite chemical potential or baryon number density, we note that it is sufficient to turn on the time component of the gauge field, A_t . By symmetry considerations, we then take $A_t = A_t(r)$, corresponding to the world volume electric field.

Therefore, we will consider the ansatz for the D5-brane world volume field of the form $\phi(r, t) = \omega t + f(r)$, with other directions fixed, but now $F_{ab} = F_{rt} = \partial_r A_t(r)$. Using this ansatz and the metric (2.5) in terms of (2.4), it is easy to derive the components of the induced world volume metric on the D5-brane, g_{ab}^{D5} , and compute the determinant, $\det g_{ab}^{D5}$, resulting the DBI action (2.6), as:

$$S_{D5} \simeq -T_{D5} \int dr dt r \sqrt{1 + \frac{r^2(\phi')^2}{6} - \frac{L^4 \dot{\phi}^2}{6r^2} - (A'_t)^2}. \quad (4.1)$$

Here we note that by setting $\dot{\phi} = \omega = A'_t(r) = 0$, our action (4.1) reduces to that of the probe D5-brane action in the BKS model, (2.7). As in the BKS model reviewed in Sec. 2, we restrict brane motion to the ϕ -direction of the transverse S^2 sphere and fix other directions constant. Thus, in our set-up we let, in addition, the probe rotate about the S^2 , as before, and furthermore turn on a non-constant world-volume electric on the probe.

The D5-brane equation of motion from the action (4.1) is:

$$\frac{\partial}{\partial r} \left[\frac{r^3 \phi'}{\sqrt{1 + \frac{r^2(\phi')^2}{6} - \frac{L^4 \dot{\phi}^2}{6r^2} - (A'_t)^2}} \right] = \frac{\partial}{\partial t} \left[\frac{L^4 \dot{\phi}}{r \sqrt{1 + \frac{r^2(\phi')^2}{6} - \frac{L^4 \dot{\phi}^2}{6r^2} - (A'_t)^2}} \right], \quad (4.2)$$

$$\frac{\partial}{\partial r} \left[\frac{r A'_t}{\sqrt{1 + \frac{r^2(\phi')^2}{6} - \frac{L^4 \dot{\phi}^2}{6r^2} - (A'_t)^2}} \right] = 0. \quad (4.3)$$

By taking the large radii limit, $r \rightarrow \infty$, it is straightforward to see that Eq. (4.3) implies $A'_t \simeq a_B/r$, with a_B denoting the VEV of baryon density number.

Take rotating solutions to (4.2) of the form:

$$\phi(r, t) = \omega t + f(r), \quad f(r) = \sqrt{6} r_0^2 \int_{r_0}^r \frac{dr}{r} \sqrt{\frac{1 - L^4 \bar{\omega}^2 / r^2 - (A'_t)^2}{r^4 - r_0^4}}. \quad (4.4)$$

Here we set $\bar{\omega} = \omega/\sqrt{6}$ and note that when $\omega = A_t(r) = 0$, our solution (4.4) integrates to that of probe D5-brane in the BKS model, [28], reviewed in Sec. 2, with the probe wrapping $adS_3 \times S^3$ in $adS_5 \times T^{1,1}$ (see Eq. (2.10)). The solution (4.4) is parameterized by (r_0, ω, a_B) and describes probe D5-brane motion, with non-constant world volume gauge field $A_t(r)$ and angular velocity ω about the transverse $S^2 \subset T^{1,1}$, starting and ending up at the boundary. The probe descends from the UV boundary at infinity to the minimal extension r_0 in the IR where it bends back up the boundary. We also note that inspection of (4.4) illustrates, in the limit $r \rightarrow$ large, that the behavior of $df(r)/dr = f_r(r)$ does not depend on ω and a_B (see Fig. 3). This illustrates that in the large radii limit the solution $f(r)$ in (4.4) gives the world volume field $\phi(r)$ of the BKS model (see Sec. 2) with the boundary values ϕ_{\pm} in the asymptotic UV limit, $r \rightarrow \infty$ (see also Fig. 3). But, we note that in the (other) IR limit, i.e., when $r \rightarrow$ small, the behavior of $f_r(r)$ does depend on ω . Furthermore, we note here that by turning on, in addition, the world volume electric field merely changes the scale but leaves the behavior of $f_r(r)$ in the IR unchanged. Inspection of (4.4) illustrates that in the IR the behavior of $f_r(r)$ with $\omega > 0$ is comparable to that of with $\omega = 0$, only if certain $\omega > 0$ are chosen. (see Fig. 3). This illustrates that in the small radii limit in the IR the behavior of $f_r(r)$ (here) does compare to that of $\phi'(r) = d\phi/dr$ in the BKS (see Sec. 2),—with $\phi'(r) \rightarrow \infty$ in the IR limit $r \rightarrow r_0^-$, consistent with U-like embedding, only if certain $\omega > 0$ are chosen.

To derive the induced metric on the D5-brane, we put the rotating solution (4.4) into the background metric (2.5) in terms of (2.4) and obtain:

$$\begin{aligned}
ds_{D5}^2 = & -\frac{(3r^2 - L^4\omega^2)}{3L^2}dt^2 + \frac{L^2}{r^2} \left[\frac{3r^2(r^4 - r_0^4) + r_0^4(6r^2(1 - (A'_t)^2) - L^4\omega^2)}{3r^2(r^4 - r_0^4)} \right] dr^2 \\
& + \frac{2L^2\omega r_0^2}{3r^2} \sqrt{\frac{6r^2(1 - (A'_t)^2) - L^4\omega^2}{r^4 - r_0^4}} dr dt + \frac{r^2}{L^2} dx^2 \\
& + \frac{L^2}{3} \left[\frac{1}{2}(\Omega_1^2 + \Omega_2^2) + \frac{1}{3}\Omega_3^2 + \omega\Omega_1 dt - \frac{r_0^2}{r^2} \sqrt{\frac{6r^2(1 - (A'_t)^2) - L^4\omega^2}{r^4 - r_0^4}} \Omega_1 dr \right].
\end{aligned} \tag{4.5}$$

Here we note that by setting $\omega = A_t = 0$, our induced world volume metric (4.5) reduces to that of the BKS model, [28], reviewed in Sec. 2. In this case, for $r_0 = 0$ the induced world volume metric is that of $adS_3 \times S^3$ and the dual gauge theory describes the conformal and chiral symmetric phase. On contrary, for $r_0 > 0$ the induced world volume metric has no adS factor and the conformal invariance of the dual gauge theory must be broken in such case. In order to find the world volume horizon and Hawking temperature, we first eliminate the relevant cross term. To eliminate the relevant cross-term in (4.5), we consider a coordinate transformation:

$$\tau = t - \omega L^4 r_0^2 \int \frac{dr (6r^2(1 - (A'_t(r))^2) - L^4\omega^2)^{1/2}}{r^2(3r^2 - L^4\omega^2)(r^4 - r_0^4)^{1/2}}. \tag{4.6}$$

The induced metric on the rotating D5-brane, (4.5), then takes the form:

$$\begin{aligned}
ds_{D5}^2 = & -\frac{(3r^2 - L^4\omega^2)}{3L^2}d\tau^2 \\
& + \frac{L^2}{r^2} \left[\frac{(3r^2 - L^4\omega^2)(r^4 - r_0^4) + r_0^8(6r^2(1 - (A'_t)^2) - L^4\omega^2)}{(3r^2 - L^4\omega^2)(r^4 - r_0^4)} \right] dr^2 \\
& + \frac{r^2}{L^2} dx^2 + -\frac{L^2}{3} \left[\frac{1}{2}(\Omega_1^2 + \Omega_2^2) + \frac{1}{3}\Omega_3^2 \right] \\
& - \frac{L^2}{3} \left[\omega\Omega_1 d\tau + \frac{3r_0^2}{3r^2 - L^4\omega^2} \sqrt{\frac{6r^2(1 - (A'_t)^2) - L^4\omega^2}{r^4 - r_0^4}} \Omega_1 dr \right].
\end{aligned} \tag{4.7}$$

Here we note that for $r_0 = 0$ the induced world volume metric (4.7) has no horizon solving $-g_{\tau\tau} = g^{rr} = 0$, and thus not given by the black hole geometry. On contrary, for $r_0 > 0$ the induced world volume horizon solves the equation:

$$H(r) = r^2(r^4 - r_0^4)(3r^2 - L^4\omega^2) = 0. \tag{4.8}$$

Eq.(4.8) contains two real positive definite zeros (see also Fig.3). The thermal horizon of the induced world volume black hole geometry is given by the zero $3r_H^2 - L^4\omega^2 = 0$, with the horizon varying continuously with varying the angular velocity

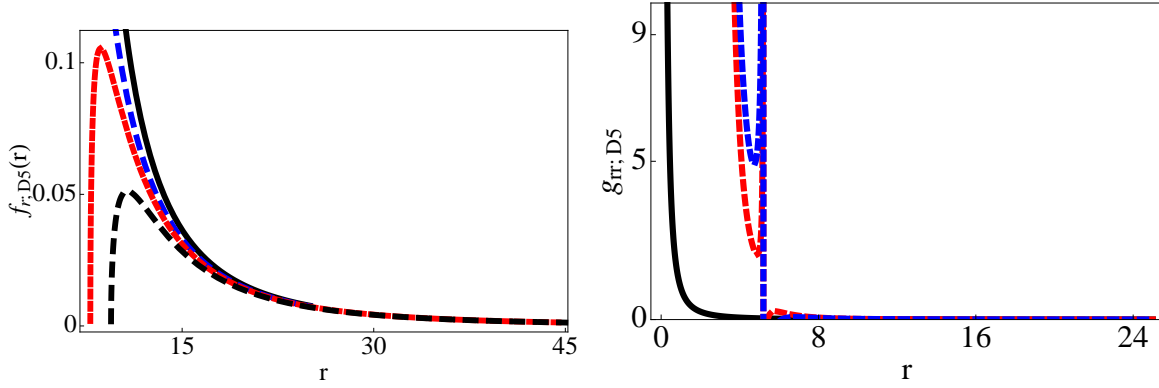


Figure 3: [Left] The behavior of the derivative of the world volume field with respect to r with $L = 1, r_0 = 7, \omega = 0, a_B = 0$ (black-solid), $\omega = 5, a_B = 4$ (blue-dashed), $a_B = 6$ (red-dashed), and $a_B = 8$ (black-dashed). [Right] The behavior of the g_{rr} component of the induced world volume metric with $L = 1, r_0 = \omega = a_B = 0$ (black-solid), $r_0 = 3, \omega = 9, a_B = 4$ (red-dashed), and $a_B = 5$ (blue-dashed).

ω , as expected. Eq. (4.8) also shows that the horizon must grow from the minimal extension $r_0 \neq 0$ with increasing the angular velocity ω , as before. We thus conclude at this point that when r_0 is positive definite ($r_0 > 0$) and spin is turned on ($\omega > 0$), the induced world volume metric on the rotating probe D5-brane wrapping $adS_3 \times S^3$ in $adS_5 \times T^{1,1}$ admits a thermal horizon growing continuously with increasing the angular velocity, regardless of the presence of the world volume gauge electric field.

The Hawking temperature on the probe D5-brane can be found from the induced world-volume metric (4.7) in the form:

$$T_{H,D5} = \frac{(g^{rr})'}{4\pi} \Big|_{r=r_H} = \frac{3r_H^3(r_H^4 - r_0^4)}{2\pi L^2 r_0^4 [6r_H^2(1 - (A'_t)^2) - L^4 \omega^2]} = \frac{r_H^3(r_H^4 - r_0^4)}{2\pi L^2 r_0^4 (r_H^2 - 2a_B^2)}. \quad (4.9)$$

Here, we note that from (4.9) that when the world volume horizon is at the minimal radial extension, $r_H = r_0$, the Hawking temperature of the world volume black hole geometry is identically zero, $T_{H,D5} = 0$. The Hawking temperature (4.9) of the world-volume black hole solution (4.7) also has a number of interesting features, which depend on the choice of parameters $\{a_B, r_0, \omega\}$. Therefore we note the following points:

- For $a_B = 0, r_0 = 4$ and $\omega \geq 0$, the world-volume Hawking temperature $T_{H,D5}$ (4.7) increases monotonically with increasing the angular velocity ω , by which the world-volume horizon size r_H grows (see Fig. 4). In this case, changing r_0 changes the scale, but not the behavior of the temperature (4.9). In particular, inspection of (4.9) shows that decreasing/increasing r_0 increases/decreases the temperature and produces relatively large hierarchies between temperature scales, $T_{H,D5}(r_0 < 1)/T_{H,D5}(r_0 > 1) \simeq$

10^4 , while the temperature behavior remains unchanged (see Fig. 4).

- For $0 < a_B \leq 15$, $r_0 = 4$ and $\omega \geq 0$, the world-volume Hawking temperature $T_{H;D5}$ (4.9) no longer behaves monotonically with growing the horizon size r_H (see Fig. 4). Instead, the temperature of the solution (4.9) admits three distinct branches, including two obvious classes of black hole solutions. The first branch appears once the horizon starts to grow from the minimal extension. In this case, the temperature $T_{H;D5}$ (4.9) decreases almost immediately to negative values before peeking off very sharply, producing a divergent-like behavior, hitting zero, and then growing into positive values (see Fig. 4). The second branch appears once the horizon continues to grow, away from the zero point. In this case, the temperature $T_{H;D5}$ (4.9) decreases to positive values, in an ‘inverse-like’ manner with the horizon, before reaching its non-zero minimum (see Fig. 4). Therefore in the neighborhood of the zero point the world-volume temperature of the solution decreases with increasing horizon size. These ‘small’ black holes have the familiar behavior of five-dimensional black holes in asymptotically flat spacetime, since their temperature decreases with increasing horizon size r_H . The third branch appears once the horizon continues to grow from its radius setting the non-zero minimum of $T_{H;D5}$. In this case, the other class of black hole solution appears with its temperature only increasing with increasing horizon size r_H , like ‘large’ black holes (see Fig. 4). This behavior is like that of the temperature with $a_B = 0$, however, in the latter two branches, the temperature of the black hole solution scales higher than that of with $a_B = 0$ (see Fig. 4). It is thus remarkable that by varying a_B , the scale and behavior of the temperature changes continuously with growing horizon size r_H (see Fig. 4). It is clear that by increasing/decreasing a_B the temperature behavior changes dramatically, while the temperature scales change very moderately, producing only small hierarchies, $T_{H;D5}(a_B <)/T_{H;D5}(a_B >) \simeq 0.5$ (see Fig. 4).

- By varying r_0 , while keeping the other parameters within the above range, only the scale but not the behavior of the temperature of the black hole solution, $T_{H;D5}$ (4.9), changes. For both $r_0 < 1$ and $r_0 > 1$, i.e., $r_0 \simeq 8$, only the temperature scale changes, and the temperature behavior remains unchanged. In this latter case, the temperature scales less than in previous cases ($r_0 > 1$), increases with increasing a_B as before, and behaves as before, increasing and decreasing continuously with growing r_H (see Fig. 4). In this latter case, therefore there are still two branches, corresponding to two classes of black hole solutions, including both ‘large’ and ‘small’ black holes, with temperature scales setting relatively small hierarchies, $T_{H;D5}(r_0 <)/T_{H;D5}(r_0 >) \simeq 10$.

We therefore conclude at this point that when the minimal extension changes, the temperature scale of the world volume black hole solution changes dramatically and sets large hierarchies, while the temperature behavior remains unchanged. We conclude, however, that when the world volume electric field is turned on, the temperature behavior changes dramatically and includes two distinct branches corresponding

to ‘large’ and ‘small’ black hole solutions, respectively, while the temperature scale changes moderately and thereby sets only moderate hierarchies. In this case, we also conclude that when, in addition, the minimal extension gets increased, the temperature behavior remains unchanged and includes the same two branches corresponding to ‘large’ and ‘small’ black hole solutions, with the temperature scales setting relatively small hierarchies.

We further notice that by taking into account the backreaction of the above solution to the KW gravity dual, $adS_5 \times T^{1,1}$, one accordingly awaits the D5-brane to form a mini black hole in KW, corresponding to a locally thermal gauge field theory in the probe limit. Thereby, the rotating D5-brane describes a thermal object in the dual gauge field theory. In the KW example here, the configuration is dual to $\mathcal{N} = 1$ gauge theory coupled to a defect flavor subject to an external electric field. As the gauge theory itself is at zero temperature as the defect flavor is at finite temperature, given by (4.9), we conclude that the configuration describes non-equilibrium steady state. However, as we shall show below, the energy from the flavor sector will in the end dissipate to the gauge theory.

So far, in this example, we neglected the backreaction of the D5-brane to the KW gravity dual, as we worked in the probe limit. It is useful to observe the extend this is justifiable. To this end, we derive the components of the energy–stress tensor of the D5-brane, which take the form:

$$\begin{aligned}\sqrt{-g}J_{t;D5}^t &\equiv \frac{\tilde{T}_{D5} r(1 + r^2(\phi')^2/6)}{\sqrt{1 + r^2(\phi')^2/6 - L^4\dot{\phi}^2/6r^2 - (A')^2}} \\ &= \frac{\tilde{T}_{D5}(r^6 - r_0^4(L^4\bar{\omega}^2 + a_B^2))}{r^2\sqrt{(r^4 - r_0^4)(r^2 - L^4\bar{\omega}^2 - a_B^2)}},\end{aligned}\tag{4.10}$$

$$\begin{aligned}\sqrt{-g}J_{r;D5}^r &\equiv -\frac{\tilde{T}_{D5} r(1 - L^4\dot{\phi}^2/6r^2)}{\sqrt{1 + r^2(\phi')^2/6 - L^4\dot{\phi}^2/6r^2 - (A')^2}} \\ &= -\tilde{T}_{D5}(r^2 - L^4\bar{\omega}^2)\sqrt{\frac{r^4 - r_0^4}{r^2 - L^4\bar{\omega}^2 - a_B^2}},\end{aligned}\tag{4.11}$$

$$\sqrt{-g}J_{t;D5}^r \equiv \frac{\tilde{T}_{D5} r^3 \dot{\phi} \phi'}{\sqrt{1 + r^2(\phi')^2/6 - L^4\dot{\phi}^2/6r^2 - (A')^2}} = \tilde{T}_{D5} r_0^2 \bar{\omega}.\tag{4.12}$$

Using (4.10)–(4.12), we can derive the total energy and energy flux of the D-brane system. The total energy of the D5-brane in the above configuration is given by:

$$E_{D5} = \tilde{T}_{D5} \int_{r_0}^{\infty} \frac{dr (r^6 - r_0^4(L^4\bar{\omega}^2 + a_B^2))}{r^2\sqrt{(r^4 - r_0^4)(r^2 - L^4\bar{\omega}^2 - a_B^2)}}.\tag{4.13}$$

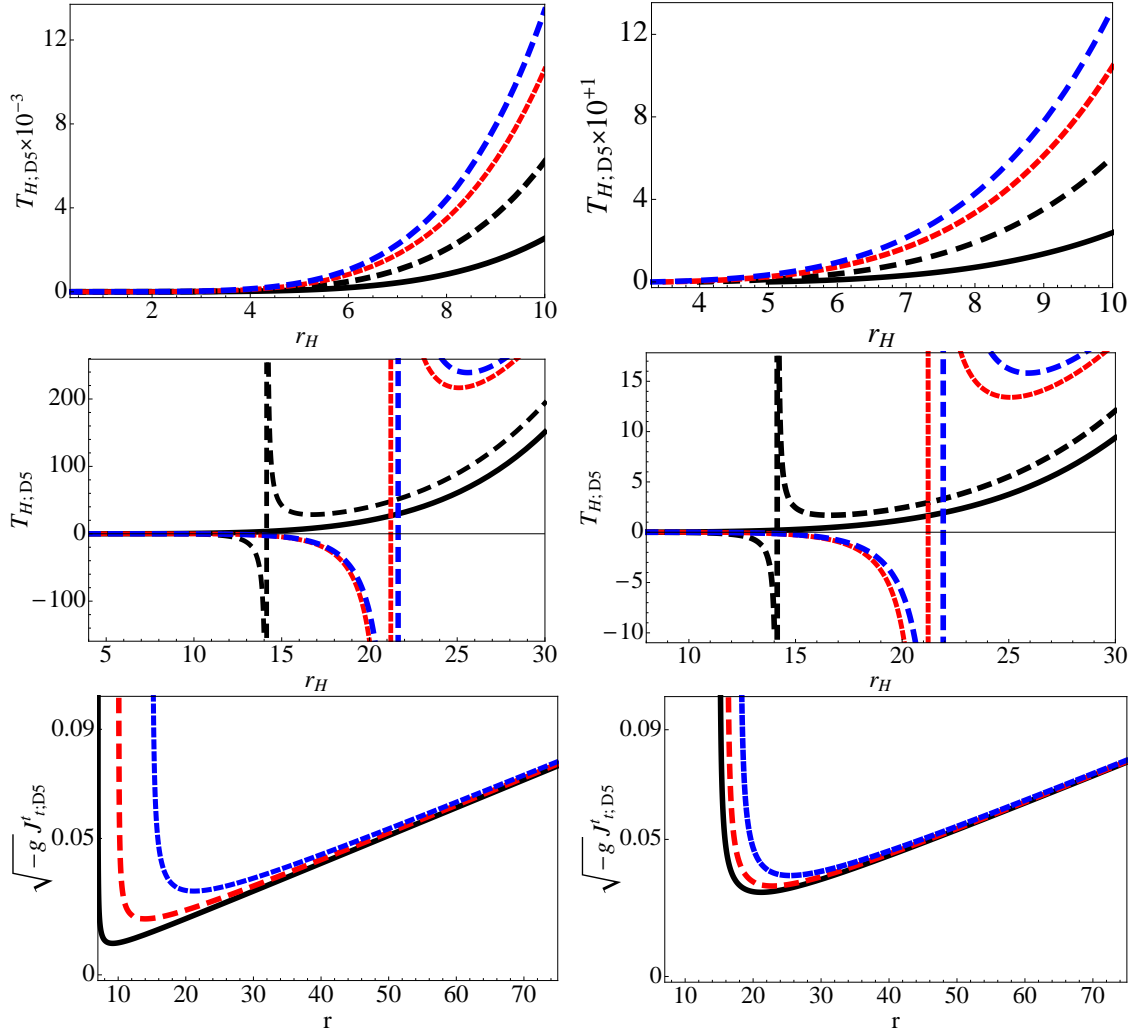


Figure 4: [Up-Left] The behavior of the world volume Hawking temperature with $r_0 = 0.5$ (black-solid), $r_0 = 0.4$ (black-dashed), $r_0 = 35$ (red-dashed), $r_0 = 0.33$ (blue-dashed), $a_B = 0$, and $L = 10$. [Up-Right] The behavior of the temperature with $r_0 = 5$ (black-solid), $r_0 = 4$ (black-dashed), $r_0 = 3.5$ (red-dashed), $r_0 = 3.3$ (blue-dashed), $a_B = 0$, and $L = 10$. [Middle-Left] The behavior of the temperature with $a_B = 0$ (black-solid), $a_B = 10$ (black-dashed), $a_B = 15$ (red-dashed), $r_0 = 15.5$ (blue-dashed), $r_0 = 4 = 0$, and $L = 10$. [Middle-Right] The behavior of the temperature with $a_B = 0$ (black-solid), $a_B = 10$ (black-dashed), $a_B = 15$ (red-dashed), $r_0 = 15.5$ (blue-dashed), $r_0 = 8$, and $L = 10$. [Down-Left] The behavior of the energy-density, $\sqrt{-g}J^t_{r;D5}$, with $\omega = 1$ (black-solid), $\omega = 6$ (blue-dashed), $\omega = 10$ (red-dashed), $a_B = 15$ and $r_0 = 7$. [Down-Right] The behavior of the energy-density with $a_B = 0$ (black-solid), $a_B = 10$ (blue-dashed), $a_B = 15$ (red-dashed), $\omega = 1$, and $r_0 = 7$. In all cases, $L = \alpha' = 1$ and $g_s = 0.1$.

Taking the limit $r \rightarrow r_0$, Eq.(4.10) shows that the energy density of the (defect) flavor brane, the integrand in (4.13), enlarges dramatically, and blows up exactly

at the minimal extension, $r = r_0$, at the IR scale of conformal and chiral flavor symmetry breakdown. Therefore, we conclude that at the IR scale of symmetries breakdown, $r = r_0$, the backreaction of the D5-brane to the gravity dual metric is large and cannot be neglected and forms a localized black hole centered at the IR scale $r = r_0$ in the bulk. The size of the black hole ought to increase due to the energy injected into it from the D5-brane continuously. By using the components of the energy–stress tensor (4.10)–(4.12), we can find this energy flux. We notice that in the brane configuration of interest here, with $r_0 > 0$ and $\omega > 0$, the component (4.12) is positive definite and so we derive the time evolution of the total energy in the form:

$$\dot{E}_{D5} = \frac{d}{dt} \int dr \sqrt{-g} J_{t;D5}^t = \int dr \partial_r (\sqrt{-g} J_{t;D5}^r) = \sqrt{-g} J_{t;D5}^r|_{r=r_0}^\infty = \tilde{T}_{D5} r_0^2 \bar{\omega} - \tilde{T}_{D5} r_0^2 \bar{\omega} = 0. \quad (4.14)$$

Relation (4.14) shows that, independent from the presence of the world volume electric field, the energy per unit time injected at the boundary $r = \infty$ by some external system equals the energy dissipated from the IR into the bulk, despite the total energy is time-independent, as before. This dissipation of energy from the D5-brane to the bulk will create a localized black hole in the bulk. Given this flow of energy from the probe to the bulk, we thereby conclude by duality that the energy from the defect flavor sector will in the end dissipate into the gauge theory, independent from the electric field. The injection of energy can also be seen clearly in our stationary solution by introducing cut offs, as before. We can, again, introduce UV and IR cut offs to the D5-brane solution, such that it extends from $r = r_{\text{IR}} = r_0$ to $r = r_{\text{UV}} \gg r_{\text{IR}}$. It is clear from (4.12) that, again, at both r_{IR} and $r = r_{\text{UV}}$ we have $J_t^r > 0$. This shows the presence of equal energy flux incoming from $r = r_{\text{UV}}$ and outgoing at $r = r_{\text{IR}}$ at which the energy gets not reflected back but its backreaction will nucleate a localized black hole intaking the injected energy, independent from the electric field, as before.

The energy–density (4.10) of the world-volume black hole solution (4.7) has a number of interesting features. These depend on the choice of parameters $\{r_0, a_B, \omega\}$, and therefore we note the following points.

- Increasing ω , while keeping the other parameters fixed, leaves the behavior of the energy density unaltered, increases the scale of the minimum energy-density near the IR scale, but leaves the scale of energy density more or less unaltered away from the IR scale (see Fig. 4). However, the increase in the energy-density is, so that the backreaction remains negligibly small away from the blowing up point, located at the IR scale r_0 (see Fig. 4).
- Increasing a_B , while keeping other parameters fixed, only shifts the minimum of the density and leaves the scale and behavior of the density unaltered (see Fig. 4).
- Increasing/decreasing r_0 , while keeping the other parameters fixed, leaves the scale

and behavior of the energy-density unaltered (as in Fig. 4).

In all cases, the energy-density falls sharply from its infinite value at the IR scale to its minimum value, whereupon it increases to finitely small values away from the IR scale. We thus conclude that altering the parameters of the theory yields almost no alteration in the scale and behavior of the energy-density, meaning that the density blows up at the IR scale, whereat the backreaction is non-negligible, and staying finitely small away from the IR scale, where the backreaction can be neglected.

5. Induced metric and temperature on U-like embedded probe D5-brane wrapping $adS_4 \times S^2 \subset adS_5 \times T^{1,1}$ and spinning about $S^3 \subset T^{1,1}$

As third example in our study, in this section, we continue with our analysis of the U-like embedded probe D5-brane and consider, instead, the probe wrapping $adS_4 \times S^2$ in $adS_5 \times T^{1,1}$ reviewed in Sec. 2, and turn on, in addition, spin degrees of freedom. Using spherical symmetry, we allow in our setup, the probe to rotate about the ψ -direction of the transverse S^3 with conserved angular momentum. Thus, in our setup, we allow ψ to have, in addition, time-dependence, so that $\dot{\psi}(r, t) = \omega = const.$, with ω denoting the angular velocity of the probe. This way, we construct rotating solutions. Hence, the world-volume field is given by $\psi(r, t)$, with other directions fixed.

Therefore, we may consider an ansatz for the D5-brane world volume fields θ , $\psi(r, t) = \omega t + f(r)$, and $F_{ab} = 0$. Using this ansatz and the metric (2.5) in terms of (2.3), it is easy to derive the components of the induced world volume metric on the D5-brane, g_{ab}^{D5} , and compute the determinant, $\det g_{ab}^{D5}$, resulting the DBI action (2.6) of the form:

$$S_{D5} \simeq -T_{D5} \int dr dt r^2 \sqrt{1 + \frac{r^2(\psi')^2}{9} - \frac{L^4 \dot{\psi}^2}{9r^2}}. \quad (5.1)$$

Here we note that by setting $\dot{\psi} = \omega = 0$, our action (5.1) reduces to that of the probe D5-brane action in the BKS model, (2.11). As in the BKS model reviewed in Sec. 2, restrict brane motion to the ψ -direction of the transverse S^3 sphere and fix other directions constant. Thus, in our set up we let, in addition, the probe rotate about the S^3 . The equation of motion from the action (5.1) is:

$$\frac{\partial}{\partial r} \left[\frac{r^4 \psi'}{\sqrt{1 + \frac{r^2(\psi')^2}{9} - \frac{L^4 \dot{\psi}^2}{9r^2}}} \right] = \frac{\partial}{\partial t} \left[\frac{L^4 \dot{\psi}}{\sqrt{1 + \frac{r^2(\psi')^2}{9} - \frac{L^4 \dot{\psi}^2}{9r^2}}} \right]. \quad (5.2)$$

Take rotating solutions to (5.2) of the form:

$$\psi(r, t) = \omega t + f(r), \quad f(r) = r_0^3 \int_{r_0}^r \frac{dr}{r^2} \sqrt{\frac{r^2 - L^4 \bar{\omega}^2}{r^6 - r_0^6}}. \quad (5.3)$$

Here we set $\bar{\omega} = \omega/3$ and note that when $\omega = 0$, our solution (5.3) integrates to that of probe D5-brane in the BKS model, [28], reviewed in Sec. 2, with the probe wrapping $adS_4 \times S^2$ in $adS_5 \times T^{1,1}$ (see Eq. (2.12)). The solution (5.3) is parameterized by (ω, r_0) and describes probe D5-brane motion, with angular velocity ω about the transverse $S^3 \subset T^{1,1}$, starting and ending up at the boundary. The probe descends from the UV boundary at infinity to the minimal extension r_0 in the IR where it bends back up the boundary. We also note that inspection of (5.3) illustrates, in the limit $r \rightarrow \text{large}$, that the behavior of $df(r)/dr = f_r(r)$ does not depend on ω (see Fig. 5). This illustrates that in the large radii limit the solution $f(r)$ in (5.3) gives the world volume field $\psi(r)$ of the BKS model (see Sec. 2) with the boundary values ψ_{\pm} in the asymptotic UV limit, $r \rightarrow \infty$ (see also Fig. 5). But, we note that in the (other) IR limit, i.e., when $r \rightarrow \text{small}$, the behavior of $f_r(r)$ does depend on ω . Inspection of (5.3) illustrates that in the IR the behavior of $f_r(r)$ with $\omega > 0$ is comparable to that of with $\omega = 0$, only if certain $\omega > 0$ are chosen. (see Fig. 5). This illustrates that in the small radii limit in the IR the behavior of $f_r(r)$ (here) does compare to that of $\psi'(r) = d\phi/dr$ in the BKS model (see Sec. 2),—with $\psi'(r) \rightarrow \infty$ in the IR limit $r \rightarrow r_0^-$, consistent with U-like embedding, only for certain $\omega > 0$.

To derive the induced metric on the D5-brane, we put the rotating solution (5.3) into the background metric (2.5) and obtain:

$$dS_{D5}^2 = -\frac{1}{L^2}(r^2 - L^4 \bar{\omega}^2)dt^2 + \frac{L^2}{r^2} \left[\frac{r^8 - r_0^6 L^4 \bar{\omega}^2}{r^2(r^6 - r_0^6)} \right] dr^2 + \frac{2L^2 r_0^3 \bar{\omega}}{r^2} \sqrt{\frac{r^2 - L^4 \bar{\omega}^2}{r^6 - r_0^6}} dr dt + \frac{r^2}{L^2} (dx_1^2 + dx_2^2). \quad (5.4)$$

Here we note that by setting $\omega = 0$, our induced world volume metric (5.4) reduces to that of the BKS model, [28], reviewed in Sec. 2. In this case, for $r_0 = 0$ the induced world volume metric is that of $adS_4 \times S^2$ and the dual gauge theory describes the conformal and chiral symmetric phase. On contrary, for $r_0 > 0$ the induced world volume metric has no adS factor and the conformal invariance of the dual gauge theory must be broken in such case.

In order to find the world volume horizon and Hawking temperature, we first eliminate the relevant cross term. To eliminate the relevant cross-term in (5.4), we consider a coordinate transformation:

$$\tau = t - L^4 \bar{\omega} r_0^3 \int \frac{dr}{r^2 \sqrt{(r^2 - L^4 \bar{\omega}^2)(r^6 - r_0^6)}}. \quad (5.5)$$

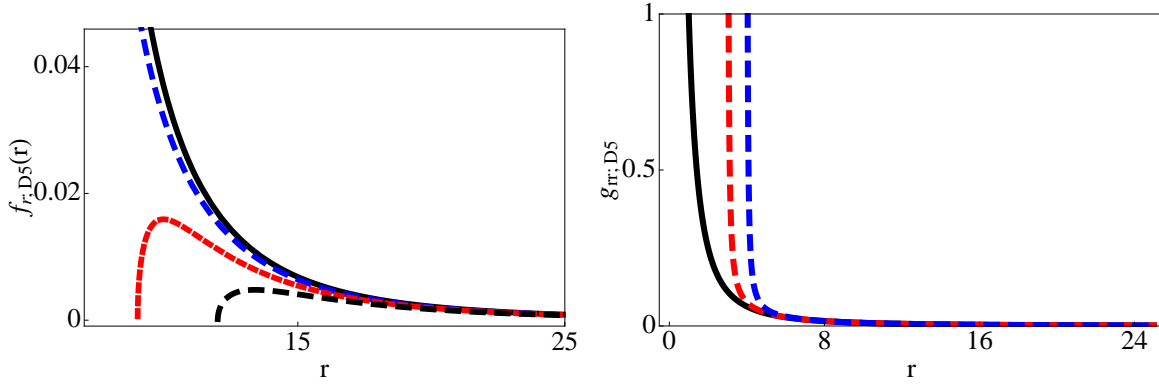


Figure 5: [Left] The behavior of the derivative of the world volume field with respect to r with $L = 1, r_0 = 7, \omega = 0$ (black-solid), $\omega = 5$ (blue-dashed), $\omega = 9$ (red-dashed), and $\omega = 12$ (black-dashed). [Right] The behavior of the g_{rr} component of the induced world volume metric with $L = 1, r_0 = 0$ (black-solid), $r_0 = 3$ (red-dashed), and $r_0 = 4$ (blue-dashed).

The induced metric on the rotating D5-brane, (5.4), then takes the form:

$$dS_{D5}^2 = -\frac{1}{L^2}(r^2 - L^4\bar{\omega}^2)d\tau^2 + \frac{L^2r^4}{r^6 - r_0^6}dr^2 + \frac{r^2}{L^2}(dx_1^2 + dx_2^2). \quad (5.6)$$

The induced world volume metric (5.6) is not given by the black hole geometry with thermal horizon solving $-g_{\tau\tau} = g^{rr}|_{r=r_H=0} = 0$. Inspection of (5.6) may seem to indicate though that for a very specific, degenerate choice of parameters, $r_0 = L^{2/3}\bar{\omega}$, the induced world volume metric (5.6) is given by the black hole geometry. But, when the embedding is fixed U-like ($r_0 > 0$), this degeneracy conflicts the continuity of the ‘would be’ world-volume thermal horizon: The ‘would be’ world volume thermal horizon, $r_H = L^2\bar{\omega}$, grows continuously with increasing the angular velocity continuously from zero, $\omega = 0$, to positive definite values, $\omega > 0$. This means that, in this limit, when $\omega = 0$, by degeneracy, the embedding is rather V-like, and only then U-like, when $\omega > 0$. Thus, in this example, there is no continuous world volume horizon consistent with the U-like embedding of the probe. We therefore conclude that the induced world volume metric on the U-like embedded probe D5-brane wrapping the $adS_4 \times S^2$ spacetime (in the BKS model) and rotating about the transverse $S^3 \subset T^{1,1}$ does not describe the world volume black hole geometry with thermal horizon and Hawking temperature of expected features.

6. Induced metric and temperature on U-like embedded probe D3-brane wrapping $adS_2 \times S^2 \subset adS_5 \times T^{1,1}$ and spinning about $S^3 \subset T^{1,1}$

As fourth and final example in our study, in this section, we consider another type of probe, namely, the U-like embedded probe D3-brane wrapping $adS_2 \times S^2$ in $adS_5 \times T^{1,1}$ reviewed in Sec. 2, taking into account additional spin degrees of freedom. Using spherical symmetry, we allow in our setup, the probe to rotate about the ψ -direction of the transverse S^3 with conserved angular momentum. Thus, in our setup, we allow ψ to have, in addition, time-dependence, so that $\dot{\psi}(r, t) = \omega = \text{const.}$, with ω denoting the angular velocity of the probe. This way, we construct rotating solutions. Hence, the world-volume field is given by $\psi(r, t)$, with other directions fixed.

Thus, we consider an ansatz for the D3-brane world volume $\psi(r, t) = \omega t + f(r)$, with other directions fixed, and $F_{ab} = 0$. Using this ansatz and the metric (2.5) in terms of (2.3), it is easy to derive the components of the induced world volume metric on the D3-brane, g_{ab}^{D3} , and compute the determinant, $\det g_{ab}^{D3}$, resulting the DBI action (2.6) of the form:

$$S_{D3} \simeq -T_{D3} \int dr dt \sqrt{1 + \frac{r^2(\psi')^2}{9} - \frac{L^4 \dot{\psi}^2}{9r^2}}. \quad (6.1)$$

Here we note that by setting $\dot{\psi} = \omega = 0$, our action (6.1) reduces to that of the probe D3-brane action in the BKS model, (2.7). As in the BKS model reviewed in Sec. 2, restrict brane motion to the ψ -direction of the transverse S^3 sphere and fix other directions constant. Thus, in our set up, we let, in addition, the probe rotate about the S^3 . The equation of motion from the action (6.1) is:

$$\frac{\partial}{\partial r} \left[\frac{r^2 \psi'}{\sqrt{1 + \frac{r^2(\psi')^2}{9} - \frac{L^4 \dot{\psi}^2}{9r^2}}} \right] = \frac{\partial}{\partial t} \left[\frac{L^4 \dot{\psi}}{r^2 \sqrt{1 + \frac{r^2(\psi')^2}{9} - \frac{L^4 \dot{\psi}^2}{9r^2}}} \right]. \quad (6.2)$$

Take rotating solutions to (6.2) of the form:

$$\psi(r, t) = \omega t + f(r), \quad f(r) = 3r_0 \int_{r_0}^r \frac{dr}{r^2} \sqrt{\frac{r^2 - L^4 \bar{\omega}^2}{r^2 - r_0^2}}. \quad (6.3)$$

Here we set $\bar{\omega} = \omega/3$ and note that when $\omega = 0$, our solution (6.3) integrates to that of probe D3-brane in the BKS model, [28], reviewed in Sec. 2, with the probe wrapping $adS_2 \times S^2$ in $adS_5 \times T^{1,1}$ (see Eq. (2.14)). The solution (6.3) is parameterized by (ω, r_0) and describes probe D3-brane motion, with angular velocity ω about the transverse $S^3 \subset T^{1,1}$, starting and ending up at the boundary. The probe descends

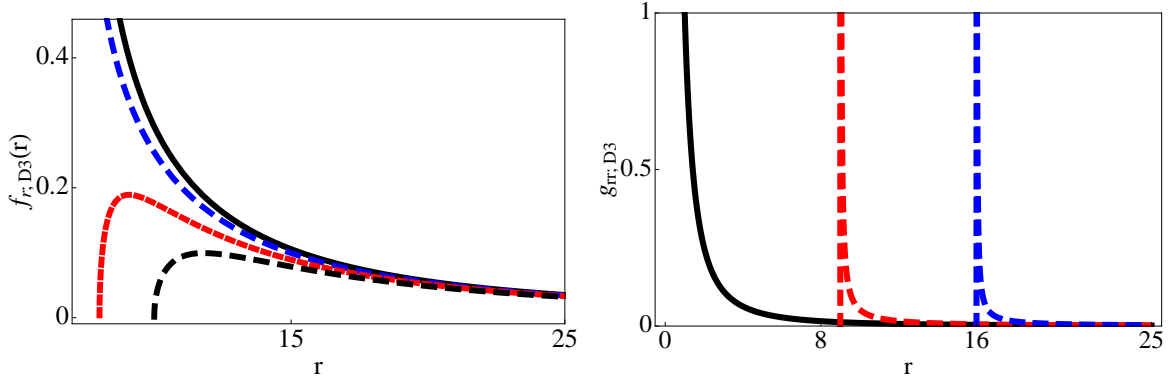


Figure 6: [Left] The behavior of the derivative of the world volume field with respect to r with $L = 1, r_0 = 7, \omega = 0$ (black-solid), $\omega = 5$ (blue-dashed), $\omega = 8$ (red-dashed), and $\omega = 10$ (black-dashed). [Right] The behavior of the g_{rr} component of the induced world volume metric with $L = 1, r_0 = 0$ (black-solid), $r_0 = 3$ (red-dashed), and $r_0 = 4$ (blue-dashed).

from the UV boundary at infinity to the minimal extension r_0 in the IR where it bends back up the boundary. We also note that inspection of (6.3) illustrates, in the limit $r \rightarrow \text{large}$, that the behavior of $df(r)/dr = f_r(r)$ does not depend on ω (see Fig. 6). This illustrates that in the large radii limit the solution $f(r)$ in (6.3) gives the world volume field $\psi(r)$ of the BKS model (see Sec. 2) with the boundary values ψ_{\pm} in the asymptotic UV limit, $r \rightarrow \infty$ (see also Fig. 6). But, we note that in the (other) IR limit, i.e., when $r \rightarrow \text{small}$, the behavior of $f_r(r)$ does depend on ω . Inspection of (6.3) illustrates that in the IR the behavior of $f_r(r)$ with $\omega > 0$ is comparable to that of with $\omega = 0$, only if certain $\omega > 0$ are chosen (see Fig. 6). This illustrates that in the small radii limit in the IR the behavior of $f_r(r)$ (here) does compare to that of $\psi'(r) = d\phi/dr$ in the BKS model (see Sec. 2),—with $\psi'(r) \rightarrow \infty$ in the IR limit $r \rightarrow r_0^-$, consistent with U-like embedding, only for certain $\omega > 0$.

To derive the induced metric on the D3-brane, we put the rotating solution (6.3) into the background metric (2.5) and obtain:

$$dS_{D3}^2 = -\frac{1}{L^2}(r^2 - L^4\bar{\omega}^2)dt^2 + \frac{L^2}{r^2} \left[\frac{r^4 - r_0^2 L^4 \bar{\omega}^2}{r^2(r^2 - r_0^2)} \right] dr^2 + \frac{2L^2 r_0 \bar{\omega}}{r^2} \sqrt{\frac{r^2 - L^4 \bar{\omega}^2}{r^2 - r_0^2}} dr dt. \quad (6.4)$$

To eliminate the cross-term in (6.4), we consider a coordinate transformation:

$$\tau = t - L^4 \bar{\omega} r_0 \int \frac{dr}{r^2 \sqrt{(r^2 - L^4 \bar{\omega}^2)(r^2 - r_0^2)}}. \quad (6.5)$$

The induced world volume metric on the rotating probe D3-brane then reads:

$$dS_{D3}^2 = -\frac{1}{L^2}(r^2 - L^4\overline{\omega}^2)d\tau^2 + \frac{L^2}{r^2 - r_0^2}dr^2. \quad (6.6)$$

The induced world volume metric (6.6) is not given by the black hole geometry with thermal horizon solving $-g_{\tau\tau} = g^{rr}|_{r=r_H} = 0$. Inspection of (6.6) may seem to indicate though that for a very specific, degenerate choice of parameters, $r_0 = L^2\overline{\omega}$, the induced world volume metric (6.6) is that of the BTZ black hole metric minus the angular coordinate. But, when the embedding is fixed U-like ($r_0 > 0$), this degeneracy is inconsistent with the continuity of the ‘would be’ world volume horizon: The ‘would be’ world volume horizon, $r_H = L^2\overline{\omega}$, has to grow continuously with increasing the angular velocity continuously, i.e., from zero, $\omega = 0$, to any positive definite values, $\omega > 0$. This implies that when $\omega = 0$, the embedding is V-like, and only then U-like, when $\omega > 0$. Thus, in this example, there is no continuous world volume horizon consistent with the U-like embedding of the probe. We therefore conclude that the induced world volume metric on the U-like embedded probe D3-brane wrapping the $adS_2 \times S^2$ spacetime (in the BKS model) and rotating about the transverse $S^3 \subset T^{1,1}$ does not describe the world volume black hole geometry with thermal horizon and Hawking temperature of expected features.⁹

7. Discussion

In this work, we studied the induced world volume metrics and Hawking temperatures of all type IIB rotating probe flavor Dp -branes ($p = 3, 5, 7$) in the holographic BKS models. Furthermore, we studied the related energy–stress tensors and energy flow of the rotating probes in these holographic BKS models. By gauge/gravity duality, the Hawking temperatures of such U-like embedded rotating probes in the gravity dual correspond to the temperatures of flavors at finite R–charge in the (d)CFT – the gauge theory conformal and chiral flavor symmetry breakdown, and the energy flow from the thermal probes into the system, to the energy dissipation from the flavor sector into the gauge theory conformal and chiral flavor symmetry breakdown. Such non-equilibrium finite-spin systems and their energy flow have been previously studied in the literature in the Kuperstein–Sonnenschein holographic model, including U-like embedded spacetime filling probe flavor D7-branes with spin in the KW gravity dual of CFT with the conformal and chiral flavor symmetry breakdown. The aim of this study was to extend and generalize such former studies to more generic holographic BKS models, including all U-like embedded type IIB probe flavor branes

⁹This is in contrast with the conformal $adS_5 \times S^5$ solution where the induced world volume metric on the rotating probe D3-brane describes the world volume black hole geometry with thermal horizon, $r_H = \omega$, and Hawking temperature, $T_H = \frac{\sqrt{3}\omega}{2\pi}$, of expected features [11].

in the KW gravity dual of (d)CFT with conformal and chiral flavor symmetry breakdown. The motivation of our study was to exemplify novel non-equilibrium systems in holographic models dual to defect gauge theories, including dCFTs with spontaneous breakdown of the conformal and chiral flavor symmetry.

We started our analysis by reviewing certain aspects of our previous case-study of U-like embedded spacetime filling probe D7-branes wrapping $adS_3 \times S^3$ in $adS_5 \times T^{1,1}$ and rotating about the trasverse $S^2 \subset T^{1,1}$ in the KW gravity dual of CFT with spontaneous conformal and chiral flavor symmetry breakdown. We showed that when the embedding is U-like, i.e., when the embedding parameter,—given by the minimal extension of the probe—, is positive definite and additional spin, is turned on, the induced world volume metric on the probe admits thermal horizons and Hawking temperatures of expected features. We found that the world volume horizon forms about the minimal extension of the probe and grows continuously with increasing the angular velocity, as expected. We found that the related world volume Hawking temperature increases continuously with increasing the angular velocity, as expected. We also found that by decreasing/increasing the minimal extension, the temperature scale increases/decreases dramatically, while the temperature behavior remains unchanged. We therefore found that varying the minimal extension sets large hierarchies of temperature scales, while leaves the temperature behavior unchanged. We found, however, that the behavior of the world volume temperature can change dramatically in the presence of the world volume gauge field. We found that when the world volume electric field is turned on, the world volume temperature admits two distinct branches. We found that there is one branch where the temperature increases and another where it decreases with growing horizon size, corresponding to ‘large’ and ‘small’ black holes, respectively. Nonetheless, we found this behavior of the world volume Hawking temperature parameter dependent – depending on the size of the minimal extension of the probe. We found that when the minimal extension is increased to relatively larger values, the temperature changes again dramatically – only increasing with growing horizon size and therefore including only one branch – corresponding only to ‘large’ black holes. By gauge/gravity duality, we thus found, in this example, that when the IR scale of conformal and chiral flavor symmetry breakdown is positive definite and the flavor sector gets, in addition, R-charged, the flavor sector of the CFT becomes thermal. By gauge/gravity duality, we also found, in this example, that the temperature of flavors with finite R-charge and density chemical potential is dramatically controlled by the IR scale of conformal and chiral flavor symmetry breakdown – giving the VEV deformations of the dual gauge theory. We then noted that by taking into account the backreaction of the above solution to the KW bulk gravity dual of CFT, one naturally expects the U-like embedded rotating D7-brane to form a mini black hole in the KW gravity dual of CFT with spontaneous breakdown of the conformal and chiral flavor symmetry, in the probe limit. Hence, we found the U-like embedded rotating probe D7-brane describing a

thermal object in the dual CFT with spontaneous conformal and chiral symmetry breakdown. In this example, the system was dual to $\mathcal{N} = 1$ gauge theory (CFT) coupled to a spacetime filling flavored quark subject to an external electric field. Since the CFT itself was at zero temperature while the flavored quark was at finite temperature, we found, in this example, that such system describes non-equilibrium steady state in the CFT – the gauge theory conformal and chiral flavor symmetry breakdown. However, by computing the energy–stress tensor of the rotating probe flavor brane, we then showed that the energy from the probe will eventually dissipate into the bulk KW, dual to energy dissipation from the flavor sector into the CFT with spontaneous conformal and chiral symmetry breakdown. We first found that, independent from the parameters choice, at the minimal extension, at the IR scale of conformal and chiral flavor symmetry breakdown, the energy density blows up and thereby showed the backreaction in the IR is non-negligible. We then showed that when the minimal extension is positive definite and spin is turned on, the energy flux is non-vanishing and found the energy can flow from the brane into the bulk, forming, with the large backreaction, a black hole in the bulk KW, independent from the electric field. We also argued how this external injection of energy may be understood in our stationary solutions. We considered UV and IR cut offs in our rotating D7-brane system and noted from the energy–stress tensor that the incoming energy from the UV equals the outgoing energy from the IR where the large backreaction forms a black hole intaking the injected energy. By gauge/gravity duality, we thus found, in this example, the energy dissipation from the flavor sector into the CFT with spontaneous conformal and chiral flavor symmetry breakdown, independent from the electric field.

We then continued our analysis by considering other examples U-like embedded type IIB probe branes with spin in the KW gravity dual of dCFT with (defect) flavors at finite R-charge and spontaneous breakdown of the conformal and chiral flavor symmetry. These included the example of probe D3-brane and the two possible examples of probe D5-branes wrapping non-trivial cycles in the KW gravity dual.

In the first example, we considered the U-like embedded probe D5-brane wrapping the $adS_3 \times S^3$ in $adS_5 \times T^{1,1}$ and rotating about the transverse space $S^2 \subset T^{1,1}$ in the KW gravity dual of dCFT with spontaneous conformal and chiral flavor symmetry breakdown. In this case, we found that the induced world volume metric on the rotating probe describes the black hole geometry despite the absence of black holes in the bulk. We showed that when the embedding is U-like, i.e., when the embedding parameter, –given by the minimal extension of the probe–, is positive definite and additional spin is turned on, the induced world volume metric on the probe admits thermal horizons and Hawking temperatures of expected features. We found that the world volume horizon forms about the minimal extension of the probe and grows continuously with increasing the angular velocity, as expected. We found that the world volume Hawking temperature increases continuously with increasing the angu-

lar velocity, as expected. We also found that by decreasing/increasing the minimal extension, the temperature scale increases/decreases dramatically, while the temperature behavior remains unchanged. We therefore found that varying the minimal extension sets large hierarchies of temperature scales, while the temperature behavior remains unchanged. We found, however, that the behavior of the world volume temperature can change dramatically in the presence of the world volume gauge electric field. We found that when the world volume electric field is turned on, the world volume temperature admits two distinct branches. We found that there is one branch where the temperature increases and another where it decreases with growing horizon size, corresponding to ‘large’ and ‘small’ black holes, respectively. We found this behavior of the world volume Hawking temperature parameter independent – independent from the size of the minimal extension of the probe. We found that when the minimal extension is increased to relatively larger values, the temperature remains unchanged – still including the two distinct branches – corresponding to ‘large’ and ‘small’ black holes, respectively. By gauge/gravity duality, we thus found, in this example, that when the IR scale of conformal and chiral flavor symmetry breakdown is positive definite and the (defect) flavor sector gets, in addition, R-charged, the (defect) flavor sector of the dCFT becomes thermal. By gauge/gravity duality, we also found, in this example, that the temperature of (defect) flavors with finite R-charge and density chemical potential is set by the baryon number density number and is almost independent from the IR scale of conformal and chiral flavor symmetry breakdown – giving the VEV deformations of the dual gauge theory. We then noted that by taking into account the backreaction of the above solution to the KW bulk gravity dual of dCFT, one naturally expects the U-like embedded D5-brane to form a mini black hole in the KW gravity dual of dCFT with spontaneous breakdown of the conformal and chiral flavor symmetry, in the probe limit. Hence, we found the U-like embedded rotating probe D5-brane describing a thermal object in the dual dCFT with spontaneous conformal and chiral symmetry breakdown. In this example, the system was dual to $\mathcal{N} = 1$ gauge theory coupled to a defect flavor (dCFT). Since the gauge theory itself was at zero temperature while the defect flavor was at finite temperature, we found, in this example, that such system describes non-equilibrium steady state in the dCFT – the defect gauge theory conformal and chiral flavor symmetry breakdown. However, by computing the energy–stress tensor of the probe, we then showed that the energy from the defect flavor sector will eventually dissipate into the gauge theory with spontaneous conformal and chiral symmetry breakdown. We first found that, independent from the parameters choice, at the minimal extension, at the IR scale of conformal and chiral flavor symmetry breakdown, the energy density blows up and thereby showed the backreaction in the IR is non-negligible. We then showed that when the minimal extension is positive definite and spin is turned on, the energy flux is non-vanishing and found the energy can flow from the brane into the bulk, forming, with the large backreaction, a localised black hole in

the bulk, independent from the electric field. We also argued how this external injection of energy may be understood in our stationary solutions. We considered UV and IR cut offs in our rotating D5-brane system and noted from the energy–stress tensor that the incoming energy from the UV equals the outgoing energy from the IR where the large backreaction forms a black hole intaking the injected energy. By gauge/gravity duality, we thus found, in this example, the energy dissipation from the defect (flavor) sector into the gauge theory with spontaneous conformal and chiral flavor symmetry breakdown, independent from the electric field.

In the second example, we considered the U-like embedded probe D5-brane wrapping the $adS_4 \times S^2$ in $adS_5 \times T^{1,1}$ and rotating about the transverse internal space $S^3 \subset T^{1,1}$ in the KW gravity dual of dCFT with spontaneous conformal and chiral flavor symmetry breakdown. On contrary with the first example, in this case, we found that the induced world volume metric on the probe D5-brane is not given by the black hole geometry, $-g_{\tau\tau} = g^{rr}|_{r=r_H} = 0$, of expected features. We first noted that in order to render the induced world volume metric of the form akin to the black hole geometry, the parameter space has to be degenerate, i.e., the minimal extension has to equal the angular velocity, $r_0 = \omega$. However, we then found, in this example, that when the embedding is U-like, $r_0 > 0$, the angular velocity, ω , cannot increase continuously, as it should – from zero to positive definite values. We thus found that the degenerate choice of parameters obstructs, in turn, the continuous growth of the ‘would be’ world volume horizon. We therefore found, in this example, that the induced world volume metric on the rotating probe does not describe the black hole geometry with thermal horizon and Hawking temperature of expected features.

In the third example, we considered the simplest example of U-like embedded probe flavor brane with additional spin, dual to defect flavors with finite R-charge and spontaneous breakdown of the conformal and chiral flavor symmetry. This included the U-like embedded probe D3-brane wrapping the $adS_2 \times S^2$ spacetime in $adS_5 \times T^{1,1}$ and rotating about the transverse space $S^3 \subset T^{1,1}$ in the KW gravity dual of dCFT with spontaneous conformal and chiral flavor symmetry breakdown. We found that the induced world volume metric on the probe D3-brane is not given by the black hole geometry, $-g_{\tau\tau} = g^{rr}|_{r=r_H} = 0$, of expected features. We first noted that in order to render the induced world volume metric of the form akin to the black hole geometry, such as BTZ minus the angular coordinate, the parameter space has to be degenerate, i.e., the minimal extension has to equal the angular velocity, $r_0 = \omega$. However, we then found, in this example, that when the embedding is U-like, $r_0 > 0$, the angular velocity, ω , cannot increase continuously, as it should – from zero to positive definite values. We thus found that the degenerate choice of parameters obstructs, in turn, the continuous growth of the ‘would be’ world volume horizon. We therefore found, in this example, that the induced world volume metric on the rotating probe does not describe the world volume black hole geometry with thermal horizon and Hawking temperature of expected features.

By comparing the world volume black hole solution of the U-like embedded rotating probe D5-brane with that of the U-like embedded rotating probe D7-brane in the KW gravity dual, we found similarities and differences in the scale and behavior of the world volume horizons and Hawking temperatures. We found, in each case, that the world volume horizon forms about the minimal extension of the probe with the world volume Hawking temperature increasing continuously with increasing the angular velocity. We also found, in each case, that the temperature scale changes dramatically with changing the minimal extension, which therefore sets large hierarchies of temperature scales. In the case of probe D7-branes, we found, however, that by varying the minimal extension, the temperature scale admits much larger hierarchies than in the case of probe D5-branes. In both cases, we found though that by varying the minimal extension the temperature behavior remains unchanged. In each case, we found, however, that when, in addition, the world volume electric field is turned on, the behavior of the world volume Hawking temperature changes dramatically – admitting two distinct branches, corresponding to ‘large’ and ‘small’ black holes, respectively. However, we found then that by varying the minimal extension of the probe, the behavior of the world volume Hawking temperature of the rotating probe D7-brane varies dramatically once again, in contrast with that of the rotating probe D5-brane. We found that by increasing the minimal extension of the probe, the temperature behavior of the rotating probe D7-brane changes once again drastically, –admitting only one branch–, corresponding to ‘large’ black holes only, while that of the rotating probe D5-brane remains unchanged, –admitting two distinct branches–, corresponding to ‘large’ as well as ‘small’ black holes, respectively, as before. For both probes, we also found that by varying the world volume electric field, via varying the baryon density number, the temperature scales admit small and comparable hierarchies. Nonetheless, we found that by changing, in addition, the minimal extension, in the case of probe D7-branes, the world volume temperature admits larger hierarchies of scales than in the case of probe D5-branes. By gauge/gravity duality, we thus found that by varying the IR scale of conformal and chiral flavor symmetry breakdown, the temperature scale of flavors at finite R-charge in the (d)CFT varies dramatically and thereby admits large hierarchies, while the temperature behavior remains unchanged. By gauge/gravity duality, we found, however, that when, in addition, the external electric field is turned on, the temperature behavior of flavors at finite R-charge and density chemical potential in the (d)CFT changes dramatically, while the temperature scale changes moderately and thereby admits moderate hierarchies. By gauge/gravity duality, we also found that by varying, in addition, the IR scale of conformal and chiral flavor symmetry breakdown, the temperature behavior of flavors at finite R-charge and baryon density chemical potential in the CFT, varies once again dramatically, in contrast with the temperature of (defect) flavors at finite R-charge and density chemical potential in the dCFT. Furthermore, by comparing the energy-stress tensors of the U-like embedded rotating

probe D5-brane with that of the U-like embedded rotating probe D7-brane, we found the scale and behavior of the energy-densities very similar. We found, in each case, that the energy-density of the rotating probe always starts from its infinite value at the minimal extension where the backreaction is non-negligible, and then settles its minimum finite value near the minimal extension, from where it eventually increases to finitely larger values away from the minimal extension. However, we found that by keeping the minimal extension fixed while varying the other parameters, in the case of probe D7-brane, the energy-density scale changes moderately away from the minimal extension, in contrast with the case of probe D5-brane where it remains more or less unchanged. Nonetheless, for both probes, we found that by varying the parameters of the solution, the energy-density behavior remains unchanged. Moreover, in both cases, we found that the energy rotating probe will eventually dissipate into the bulk, forming, with the large backreaction in the IR a (localised) black hole in the bulk. By gauge/gravity duality, we thus found, in both cases, that the energy from the (defect) flavor sector at finite R-charge and density chemical potential will finally dissipate into the $\mathcal{N} = 1$ KW gauge theory with spontaneous conformal and chiral flavor symmetry breakdown.

We conclude that when the probe embedding is U-like, the induced world volume metrics of only certain type IIB probe flavor branes with spin in the KW gravity dual of $\mathcal{N} = 1$ (d)CFT admit thermal horizons and Hawking temperatures of expected features despite the absence of black holes in the bulk. We conclude, in particular, that the world volume black hole formation on U-like embedded type IIB probe flavor branes with spin in the KW gravity dual of (d)CFT is non-trivial and depends on the world volume spacetime codimension and topology of the non-trivial internal cycle wrapped by the probe. We also conclude that when the probe embedding is U-like, the world volume Hawking temperature of the rotating black hole solution on type IIB probe flavor branes in the KW gravity dual of (d)CFT is dramatically parameter dependent. We conclude, in particular, that the world volume temperature profile of the U-like embedded probe spacetime filling flavor brane with spin in KW is freely and dramatically controlled by the embedding parameter – the minimal extension of the probe, while the world volume temperature profile of the U-like embedded probe (defect) flavor brane in KW is independent from the minimal extension and set by the world volume electric field density number. By gauge/gravity duality, we therefore conclude that when the IR scale of symmetry breakdown is positive definite and the flavor sector of the KW (d)CFT with spontaneous breakdown of the conformal and chiral flavor symmetry gets, in addition, R-charged, flavor thermalization and non-equilibrium steady state formation depends non-trivially on the type of flavors inserted to the gauge theory. By gauge/gravity duality, we also conclude that the temperature profile of the spacetime filling flavors in the KW CFT is freely and dramatically controlled by the IR scale of spontaneous conformal and chiral flavor symmetry breakdown – giving the VEV deformations of the gauge theory, while the

temperature profile of (defect) flavors in the KW dCFT is independent from the IR scale and set by the VEV of baryon number. We conclude, however, that the energy of the rotating thermal probes embedded U-like in the KW gravity dual will eventually dissipate into the bulk, forming, with the large backreaction in the IR, a (localized) black hole in the bulk. By gauge/gravity duality, we thus conclude that the energy from the (defect) flavor sector will finally dissipate into the $\mathcal{N} = 1$ KW gauge theory conformal and chiral flavor symmetry breakdown.

There are the following limitations to our work. In the examples we constructed, we were unable to fully solve the Dp -brane ($p = 3, 5, 7$) equations of motion to determine the explicit analytic form of the Dp -brane world volume scalar fields, when conserved angular motion and world volume gauge fields were turned on. Therefore, in our examples, we were not able to provide full details about the probe Dp -brane solution itself, when the angular velocity and world volume gauge fields were set non-vanishing. Nevertheless, in order to derive the induced world volume metrics and compute the induced world volume Hawking temperatures, we did not need to find the explicit form of the Dp -brane world volume scalar fields. However, in all examples we constructed, we deliberately chose ansätze of solutions and induced world volume metrics that did reproduce those of the BKS models, when we turned off the angular velocity and world volume gauge fields. Moreover, in all examples, we demonstrated that, independent from the value of angular velocity and world volume gauge fields, in the large radii limit, the radial derivatives of the world volume field in our ansätze coincide with that of vanishing angular velocity and vanishing world volume gauge fields. Thus, in all examples, in the large radii limit, our ansätze solved to the Dp -brane scalar fields with asymptotic UV boundary values of the BKS models. Furthermore, in all our examples, we demonstrated that, in the small radii limit, in the IR, for specific range of angular velocities, the radial derivatives of the world volume field in our ansätze behave as that of the BKS models, consistent with U-like embeddings.

The other important issue that we did not discuss in this work is the Goldstone boson of conformal symmetry breakdown at finite R-charge – dual to rotation. We first note that the existing models in the literature identify the Goldstone in the pure case by using very specific brane embedding configurations replacing polar with Cartesian coordinates. We then note that the brane field equations of interest here involve rotational symmetry and such are usually systematically solved in polar coordinates. We thus find the identification of the Goldstone boson at finite R-charge in the embedding configurations of the pure model ambiguous and formidable task. We suspect, however, that this issue is technically more involved and may need alternative methods of inspection that go beyond the scope of this paper.

The analysis of this work may be extended in two obvious ways. One obvious extension is to study probe flavor brane thermalization in U-like embeddings in more generic type IIB holographic models, such as the regular KS and singular KT gravity

duals of $\mathcal{N} = 1$ non-conformal gauge theories including confinement and chiral symmetry breaking, and RG flow, respectively. The other obvious extension is to study probe flavor brane thermalization in U-like embeddings of type IIA holographic BKS models based on ABJM theory. We leave these extensions for our future studies.

References

- [1] J. M. Maldacena, “The Large N limit of superconformal field theories and supergravity,” *Int. J. Theor. Phys.* **38**, 1113 (1999) [*Adv. Theor. Math. Phys.* **2**, 231 (1998)] [hep-th/9711200]. S. S. Gubser, I. R. Klebanov and A. M. Polyakov, “Gauge theory correlators from noncritical string theory,” *Phys. Lett. B* **428**, 105 (1998) [hep-th/9802109]. E. Witten, “Anti-de Sitter space and holography,” *Adv. Theor. Math. Phys.* **2**, 253 (1998) [hep-th/9802150].
- [2] M. Ammon and J. Erdmenger, “Gauge/gravity duality: Foundations and applications”, Cambridge University Press, Cambridge, (2015). H. Nastase, “Introduction to the ADS/CFT Correspondence”, Cambridge University Press, Cambridge, (2015).
- [3] A. Karch and E. Katz, “Adding flavor to AdS / CFT,” *JHEP* **0206**, 043 (2002) [hep-th/0205236].
- [4] A. Karch and L. Randall, “Localized gravity in string theory,” *Phys. Rev. Lett.* **87**, 061601 (2001) [hep-th/0105108].
- [5] A. Karch and L. Randall, “Open and closed string interpretation of SUSY CFT’s on branes with boundaries,” *JHEP* **0106**, 063 (2001) [hep-th/0105132].
- [6] M. Kruczenski, D. Mateos, R. C. Myers and D. J. Winters, “Meson spectroscopy in AdS/CFT with flavor,” *JHEP* **0307**, 049 (2003) [hep-th/0304032]. D. Mateos, R. C. Myers and R. M. Thomson, “Holographic phase transitions with fundamental matter,” *Phys. Rev. Lett.* **97**, 091601 (2006) [hep-th/0605046]. D. Mateos, R. C. Myers and R. M. Thomson, “Holographic viscosity of fundamental matter,” *Phys. Rev. Lett.* **98**, 101601 (2007) [hep-th/0610184]. S. Kobayashi, D. Mateos, S. Matsuura, R. C. Myers and R. M. Thomson, “Holographic phase transitions at finite baryon density,” *JHEP* **0702**, 016 (2007) [hep-th/0611099]. D. Mateos, S. Matsuura, R. C. Myers and R. M. Thomson, “Holographic phase transitions at finite chemical potential,” *JHEP* **0711**, 085 (2007) [arXiv:0709.1225 [hep-th]]. J. Babington, J. Erdmenger, N. J. Evans, Z. Guralnik and I. Kirsch, “Chiral symmetry breaking and pions in nonsupersymmetric gauge/gravity duals,” *Phys. Rev. D* **69**, 066007 (2004) [hep-th/0306018]. R. Apeada, J. Erdmenger, N. Evans and Z. Guralnik, “Strong coupling effective

- Higgs potential and a first order thermal phase transition from AdS/CFT duality,” *Phys. Rev. D* **71**, 126002 (2005) [hep-th/0504151]. G. Itsios, N. Jokela and A. V. Ramallo, “Collective excitations of massive flavor branes,” *Nucl. Phys. B* **909**, 677 (2016) [arXiv:1602.06106 [hep-th]].
- [7] A. Karch and A. O’Bannon, “Metallic AdS/CFT,” *JHEP* **0709**, 024 (2007) [arXiv:0705.3870 [hep-th]]. M. Ammon, J. Erdmenger, M. Kaminski and P. Kerner, “Superconductivity from gauge/gravity duality with flavor,” *Phys. Lett. B* **680**, 516 (2009) [arXiv:0810.2316 [hep-th]]. M. Ammon, J. Erdmenger, M. Kaminski and P. Kerner, “Flavor Superconductivity from Gauge/Gravity Duality,” *JHEP* **0910**, 067 (2009) [arXiv:0903.1864 [hep-th]]. N. Evans, A. Gebauer, K. Y. Kim and M. Magou, “Holographic Description of the Phase Diagram of a Chiral Symmetry Breaking Gauge Theory,” *JHEP* **1003**, 132 (2010) [arXiv:1002.1885 [hep-th]]. K. Jensen, A. Karch and E. G. Thompson, “A Holographic Quantum Critical Point at Finite Magnetic Field and Finite Density,” *JHEP* **1005**, 015 (2010) [arXiv:1002.2447 [hep-th]]. K. Jensen, A. Karch, D. T. Son and E. G. Thompson, “Holographic Berezinskii-Kosterlitz-Thouless Transitions,” *Phys. Rev. Lett.* **105**, 041601 (2010) [arXiv:1002.3159 [hep-th]]. N. Evans, A. Gebauer, K. Y. Kim and M. Magou, “Phase diagram of the D3/D5 system in a magnetic field and a BKT transition,” *Phys. Lett. B* **698**, 91 (2011) [arXiv:1003.2694 [hep-th]]. S. A. Hartnoll, J. Polchinski, E. Silverstein and D. Tong, “Towards strange metallic holography,” *JHEP* **1004**, 120 (2010) [arXiv:0912.1061 [hep-th]].
- [8] C. P. Herzog, “Lectures on Holographic Superfluidity and Superconductivity,” *J. Phys. A* **42**, 343001 (2009) [arXiv:0904.1975 [hep-th]]. S. A. Hartnoll, “Lectures on holographic methods for condensed matter physics,” *Class. Quant. Grav.* **26**, 224002 (2009) [arXiv:0903.3246 [hep-th]]. T. Faulkner, N. Iqbal, H. Liu, J. McGreevy and D. Vegh, “From Black Holes to Strange Metals,” arXiv:1003.1728 [hep-th]. J. McGreevy, “Holographic duality with a view toward many-body physics,” *Adv. High Energy Phys.* **2010**, 723105 (2010) [arXiv:0909.0518 [hep-th]]. H. Liu, J. McGreevy and D. Vegh, “Non-Fermi liquids from holography,” *Phys. Rev. D* **83**, 065029 (2011) [arXiv:0903.2477 [hep-th]]. T. Faulkner, H. Liu, J. McGreevy and D. Vegh, “Emergent quantum criticality, Fermi surfaces, and AdS(2),” *Phys. Rev. D* **83**, 125002 (2011) [arXiv:0907.2694 [hep-th]].
- [9] A. O’Bannon, “Toward a Holographic Model of Superconducting Fermions,” *JHEP* **0901**, 074 (2009) [arXiv:0811.0198 [hep-th]].
- [10] S. P. Kumar, “Spinning flavour branes and fermion pairing instabilities,” *Phys. Rev. D* **84**, 026003 (2011) [arXiv:1104.1405 [hep-th]]. N. Evans and E. Threlfall,

- “Chemical Potential in the Gravity Dual of a 2+1 Dimensional System,” *Phys. Rev. D* **79**, 066008 (2009) [arXiv:0812.3273 [hep-th]].
- [11] S. R. Das, T. Nishioka and T. Takayanagi, “Probe Branes, Time-dependent Couplings and Thermalization in AdS/CFT,” *JHEP* **1007**, 071 (2010) [arXiv:1005.3348 [hep-th]].
- [12] S. F. Taghavi and A. Vahedi, “Equilibrium Instability of Chiral Mesons in External Electromagnetic Field via AdS/CFT,” *JHEP* **1606**, 053 (2016) [arXiv:1603.09264 [hep-th]]. M. Ali-Akbari and S. F. Taghavi, “Chiral Magnetic Effect in the Anisotropic Quark-Gluon Plasma,” *JHEP* **1504**, 181 (2015) [arXiv:1408.6361 [hep-th]]. M. Ali-Akbari, H. Ebrahim and Z. Rezaei, “Probe Branes Thermalization in External Electric and Magnetic Fields,” *Nucl. Phys. B* **878**, 150 (2014) [arXiv:1307.5629 [hep-th]]. M. Ali-Akbari and H. Ebrahim, “Thermalization in External Magnetic Field,” *JHEP* **1303**, 045 (2013) [arXiv:1211.1637 [hep-th]]. M. Ali-Akbari and H. Ebrahim, “Meson Thermalization in Various Dimensions,” *JHEP* **1204**, 145 (2012) [arXiv:1203.3425 [hep-th]]. L. Shahkarami, H. Ebrahim, M. Ali-Akbari and F. Charmchi, “Far-from-equilibrium initial conditions probed by a nonlocal operator,” arXiv:1702.08482 [hep-th]. A. Hajilou, M. Ali-Akbari and F. Charmchi, “A Classical String in Lifshitz-Vaidya Geometry,” arXiv:1707.00967 [hep-th]. S. R. Das, “Holographic Quantum Quench,” *J. Phys. Conf. Ser.* **343**, 012027 (2012) [arXiv:1111.7275 [hep-th]]. M. Ali-Akbari and U. Gursoy, “Rotating strings and energy loss in non-conformal holography,” *JHEP* **1201**, 105 (2012) [arXiv:1110.5881 [hep-th]]. C. Hoyos, T. Nishioka and A. O’Bannon, “A Chiral Magnetic Effect from AdS/CFT with Flavor,” *JHEP* **1110**, 084 (2011) [arXiv:1106.4030 [hep-th]].
- [13] J. G. Russo and P. K. Townsend, “Accelerating Branes and Brane Temperature,” *Class. Quant. Grav.* **25**, 175017 (2008) [arXiv:0805.3488 [hep-th]]. M. Chernicoff and A. Guijosa, “Acceleration, Energy Loss and Screening in Strongly-Coupled Gauge Theories,” *JHEP* **0806**, 005 (2008) [arXiv:0803.3070 [hep-th]]. A. Paredes, K. Peeters and M. Zamaklar, “Temperature versus acceleration: The Unruh effect for holographic models,” *JHEP* **0904**, 015 (2009) [arXiv:0812.0981 [hep-th]]. C. Athanasiou, P. M. Chesler, H. Liu, D. Nickel and K. Rajagopal, “Synchrotron radiation in strongly coupled conformal field theories,” *Phys. Rev. D* **81**, 126001 (2010) [Erratum-ibid. *D* **84**, 069901 (2011)] [arXiv:1001.3880 [hep-th]]. E. Caceres, M. Chernicoff, A. Guijosa and J. F. Pedraza, “Quantum Fluctuations and the Unruh Effect in Strongly-Coupled Conformal Field Theories,” *JHEP* **1006**, 078 (2010) [arXiv:1003.5332 [hep-th]]. T. Hirata, S. Mukohyama and T. Takayanagi, “Decaying D-branes and Moving Mirrors,” *JHEP* **0805**, 089 (2008) [arXiv:0804.1176 [hep-th]]. T. Hirayama,

- P. W. Kao, S. Kawamoto and F. L. Lin, “Unruh effect and Holography,” Nucl. Phys. B **844**, 1 (2011) [arXiv:1001.1289 [hep-th]].
- [14] D. Kaviani and A. E. Mosaffa, “Temperature in the Throat,” Nucl. Phys. B **910**, 724 (2016) [arXiv:1503.02026 [hep-th]].
- [15] I. R. Klebanov and M. J. Strassler, “Supergravity and a confining gauge theory: Duality cascades and chiSB-resolution of naked singularities,” JHEP **0008**, 052 (2000) [arXiv:hep-th/0007191].
- [16] I. R. Klebanov and A. A. Tseytlin, “Gravity duals of supersymmetric $SU(N) \times SU(N+M)$ gauge theories,” Nucl. Phys. B **578**, 123 (2000) [hep-th/0002159].
- [17] I. R. Klebanov and E. Witten, “Superconformal field theory on three-branes at a Calabi-Yau singularity,” Nucl. Phys. B **536**, 199 (1998) [hep-th/9807080].
- [18] A. Buchel, “Finite temperature resolution of the Klebanov-Tseytlin singularity,” Nucl. Phys. B **600**, 219 (2001) [hep-th/0011146]. A. Buchel, C. P. Herzog, I. R. Klebanov, L. A. Pando Zayas and A. A. Tseytlin, “Nonextremal gravity duals for fractional D-3 branes on the conifold,” JHEP **0104**, 033 (2001) [hep-th/0102105]. S. S. Gubser, C. P. Herzog, I. R. Klebanov and A. A. Tseytlin, “Restoration of chiral symmetry: A Supergravity perspective,” JHEP **0105**, 028 (2001) [hep-th/0102172].
- [19] P. Candelas and X. C. de la Ossa, “Comments on Conifolds,” Nucl. Phys. B **342**, 246 (1990).
- [20] D. Kaviani, “D7-brane dynamics and thermalization in the Kuperstein–Sonnenschein model,” Nucl. Phys. B **919**, 142 (2017) [arXiv:1608.02380 [hep-th]].
- [21] S. Kuperstein and J. Sonnenschein, “A New Holographic Model of Chiral Symmetry Breaking,” JHEP **0809**, 012 (2008) [arXiv:0807.2897 [hep-th]].
- [22] M. Ihl, A. Kundu and S. Kundu, “Back-reaction of Non-supersymmetric Probes: Phase Transition and Stability,” JHEP **1212**, 070 (2012) [arXiv:1208.2663 [hep-th]]. M. S. Alam, V. S. Kaplunovsky and A. Kundu, “Chiral Symmetry Breaking and External Fields in the Kuperstein-Sonnenschein Model,” JHEP **1204**, 111 (2012) [arXiv:1202.3488 [hep-th]].
- [23] T. Sakai and J. Sonnenschein, “Probing flavored mesons of confining gauge theories by supergravity,” JHEP **0309**, 047 (2003) [hep-th/0305049].
- [24] A. Dymarsky, S. Kuperstein and J. Sonnenschein, “Chiral Symmetry Breaking with non-SUSY D7-branes in ISD backgrounds,” JHEP **0908**, 005 (2009) [arXiv:0904.0988 [hep-th]].

- [25] T. Sakai and S. Sugimoto, “Low energy hadron physics in holographic QCD,” *Prog. Theor. Phys.* **113**, 843 (2005) [hep-th/0412141]. T. Sakai and S. Sugimoto, “More on a holographic dual of QCD,” *Prog. Theor. Phys.* **114**, 1083 (2005) [hep-th/0507073].
- [26] P. Ouyang, “Holomorphic D7 branes and flavored N=1 gauge theories,” *Nucl. Phys. B* **699**, 207 (2004) [hep-th/0311084]. T. S. Levi and P. Ouyang, “Mesons and flavor on the conifold,” *Phys. Rev. D* **76**, 105022 (2007) [hep-th/0506021]. S. Kuperstein, “Meson spectroscopy from holomorphic probes on the warped deformed conifold,” *JHEP* **0503**, 014 (2005) [hep-th/0411097].
- [27] F. Benini, F. Canoura, S. Cremonesi, C. Nunez and A. V. Ramallo, “Unquenched flavors in the Klebanov-Witten model,” *JHEP* **0702**, 090 (2007) [hep-th/0612118]. F. Benini, F. Canoura, S. Cremonesi, C. Nunez and A. V. Ramallo, “Backreacting flavors in the Klebanov-Strassler background,” *JHEP* **0709**, 109 (2007) [arXiv:0706.1238 [hep-th]]. F. Benini, “A Chiral cascade via backreacting D7-branes with flux,” *JHEP* **0810**, 051 (2008) [arXiv:0710.0374 [hep-th]]. F. Bigazzi, A. L. Cotrone and A. Paredes, “Klebanov-Witten theory with massive dynamical flavors,” *JHEP* **0809**, 048 (2008) [arXiv:0807.0298 [hep-th]]. F. Bigazzi, A. L. Cotrone, A. Paredes and A. V. Ramallo, “The Klebanov-Strassler model with massive dynamical flavors,” *JHEP* **0903**, 153 (2009) [arXiv:0812.3399 [hep-th]].
- [28] O. Ben-Ami, S. Kuperstein and J. Sonnenschein, “On spontaneous breaking of conformal symmetry by probe flavour D-branes,” *JHEP* **1403**, 045 (2014) [arXiv:1310.8366 [hep-th]].
- [29] V. G. Filev, M. Ihl and D. Zoakos, “Holographic Bilayer/Monolayer Phase Transitions,” *JHEP* **1407**, 043 (2014) [arXiv:1404.3159 [hep-th]]. V. G. Filev, M. Ihl and D. Zoakos, “A Novel (2+1)-Dimensional Model of Chiral Symmetry Breaking,” *JHEP* **1312**, 072 (2013) [arXiv:1310.1222 [hep-th]].
- [30] O. Aharony, O. Bergman, D. L. Jafferis and J. Maldacena, “N=6 superconformal Chern-Simons-matter theories, M2-branes and their gravity duals,” *JHEP* **0810**, 091 (2008) [arXiv:0806.1218 [hep-th]].
- [31] V. G. Filev, C. V. Johnson, R. C. Rashkov and K. S. Viswanathan, “Flavoured large N gauge theory in an external magnetic field,” *JHEP* **0710**, 019 (2007) [hep-th/0701001]. V. G. Filev, “Criticality, scaling and chiral symmetry breaking in external magnetic field,” *JHEP* **0804**, 088 (2008) [arXiv:0706.3811 [hep-th]]. T. Albash, V. G. Filev, C. V. Johnson and A. Kundu, “Finite temperature large N gauge theory with quarks in an external magnetic field,” *JHEP* **0807**, 080 (2008) [arXiv:0709.1547 [hep-th]]. J. Erdmenger, R. Meyer and J. P. Shock,

- “AdS/CFT with flavour in electric and magnetic Kalb-Ramond fields,” JHEP **0712**, 091 (2007) [arXiv:0709.1551 [hep-th]].
- [32] J. Evslin and S. Kuperstein, “Trivializing and Orbifolding the Conifold’s Base,” JHEP **0704**, 001 (2007) [hep-th/0702041].
- [33] S. Nakamura and H. Ooguri, “Out of Equilibrium Temperature from Holography,” Phys. Rev. D **88**, no. 12, 126003 (2013) [arXiv:1309.4089 [hep-th]].
- [34] V. G. Filev, M. Ihl and D. Zoakos, “A Novel (2+1)-Dimensional Model of Chiral Symmetry Breaking,” JHEP **1312**, 072 (2013) [arXiv:1310.1222 [hep-th]].
- [35] D. Arean, D. E. Crooks and A. V. Ramallo, “Supersymmetric probes on the conifold,” JHEP **0411**, 035 (2004) [hep-th/0408210].